

The role of cytosolic kinases in chloroplast protein import

Dissertation der Fakultät für Biologie
der
Ludwig-Maximilians-Universität München

vorgelegt von

Ahmed Eisa

München 2019

Diese Dissertation wurde angefertigt unter Leitung von PD Dr. Serena Schwenkert an der Fakultät für Biologie der Ludwig-Maximilian-Universität München.

Erstgutachter: PD Dr. Serena Schwenkert

Zweitgutachter: Prof. Dr. Jörg Nickelsen

Tag der Abgabe: 16.10.2019

Tag der mündlichen Prüfung: 16.12.2019

Contents Page

Summary	V
Zusammenfassung	VI
Abbreviations	VII
1. Introduction	1
1.1 Preproteins Import into Chloroplast.....	1
1.2 Targeting to the Chloroplast.....	3
1.3 Plant Protein Kinases.....	5
1.4 Plant Dual Specificity Kinases.....	5
1.5 <i>Arabidopsis thaliana</i> STY Kinases	6
1.6 STY8, STY17, and STY46	7
1.7 The ACT Domain	7
1.8 ACT domain Sequence Homology and Structure	8
1.9 ACT Domain Ligand Binding Sites and Mechanism	9
2. Materials & Methods	10
2.1. Materials	10
2.1.1. Chemicals	10
2.1.1. Molecular Weight Markers and DNA Standards.....	10
2.1.2. Oligonucleotides	10
2.1.2. Plasmids	11
2.1.3. Antibodies	13
2.1.4. Kits.....	13
2.1.5. Enzymes	13
2.1.6. Protein Purification Column.....	14
2.1.7. Software.....	14
2.1.8. Bacterial Strains.....	14
2.1.9. Plants.....	14
2.2. Methods	15
2.2.1. Cloning.....	15
2.2.2. Transformation of <i>A. tumefaciens</i>	16

2.2.3.	Bacterial Growth Conditions.....	16
2.2.4.	Plant Growth Conditions	16
2.2.5.	Overexpression and purification of recombinant soluble proteins from <i>E.coli</i>	16
2.2.6.	Purification of proteins out of inclusion bodies from <i>E.coli</i>	17
2.2.7.	Isolation of proteins from <i>A. thaliana</i>	17
2.2.8.	Determination of protein concentration	17
2.2.9.	Relative molecular mass estimation by size exclusion chromatography	17
2.2.10.	Microscale Thermophoresis.....	18
2.2.11.	SDS polyacrylamide gel electrophoresis (SDS-PAGE).....	18
2.2.12.	Non-denaturing gradient gel electrophoresis (Native-PAGE)	18
2.2.13.	Semi-dry electro blot and immunodetection of proteins	18
2.2.14.	Phosphorylation Assay	19
2.2.15.	Detection of radiolabeled proteins	19
2.2.16.	<i>Arabidopsis thaliana</i> stable transformation with <i>Agrobacterium tumefaciens</i>	19
2.2.17.	Isolation of genomic DNA from <i>Arabidopsis thaliana</i>	20
2.2.18.	Quantitative RT-PCR analysis	20
2.2.19.	Transient transformation and protoplast isolation of <i>Nicotiana benthamiana</i>	20
2.2.20.	Chlorophyll Extraction.....	21
3.	Results.....	22
3.1.	Effects of Acclimation on STY kinases	22
3.1.1.	STY kinases phosphorylates nuclear encoded chloroplast precursors that associates with 14-3-3 and HSP70 chaperones.....	22
3.1.2.	High light affects precursor phosphorylation yield.....	24
3.1.3.	Kinase expression is upregulated in high light acclimation	25
3.1.4.	Double mutant shows reduced precursor phosphorylation yield.....	26
3.1.5.	Precursor phosphorylation and kinase expression is downregulated in heat acclimation	27
3.2.	Characterization of the ACT domain of STY kinases.....	29
3.2.1.	ACT domain regulates STY kinases	29
3.2.2.	STY8 is negatively regulated by Ile via the ACT domain	32
3.2.3.	ACT domain Protein alignment of STY8, STY17 and STY46 and selected proteins.....	35

3.2.4.	STY8 is negatively regulated by S-Adenosylmethionine via the ACT domain	38
3.2.5.	Conserved Glycine in the ACT domain of STY8 does not play a role in S-Adenosylmethionine sensitivity	40
3.1.1.	SAM and Ile inhibit precursor affinity and phosphorylation by STY8	41
3.1.2.	STY8 and the ACT domain form oligomers	43
3.1.3.	Generation and characterization of <i>sty8 sty46/35S:STY46ΔACT</i> deleted Arabidopsis mutant	45
3.1.4.	Deletion of the ACT domain does not effects leaf size and root length on plates	47
3.1.5.	Deletion of the ACT domain affects chlorophyll accumulation during greening	49
3.1.1.	Deletion of the ACT domain effects phosphorylation status of precursors in planta	51
4.	Discussion	52
4.1.	Role of Acclimation in protein import into chloroplast	52
4.1.1.	High Temperature decreases precursor phosphorylation yield	52
4.1.2.	Light increases precursor phosphorylation and STY kinase expression	53
4.1.3.	STY kinases phosphorylated precursors that associate with HSP70 and/or 14-3-3	53
4.2.	The role of the ACT domain in STY Kinase activity	54
4.2.1.	<i>In vitro</i> characterization of the ACT domain of STY kinase	54
4.2.1.1.	The ACT domain regulates spatial distribution and kinase activity	54
4.2.1.2.	Ile and SAM regulates kinase activity via the ACT domain	55
4.2.1.3.	ACT domain of STY8 involved in oligomerization	56
4.2.2.	<i>In vivo</i> characterization of the ACT domain of STY kinase	57
4.2.2.1.	The ACT domain influences etioplasts to chloroplast transition in cotyledons	57
4.2.2.2.	Linking SAM and Ile to Chloroplast function	58
4.2.2.3.	The role of SAM and Ile inhibits kinase activity during etioplasts to chloroplast transition in cotyledons	59
5.	Outlook	60
6.	References	61
	Acknowledgement	66

Curriculum vitae	67
Veröffentlichung	68
Eidesstattliche Versicherung	69

Summary

Chloroplasts were formed as a result of an endosymbiotic event in which an ancestral photosynthetic cyanobacterium was engulfed by a heterotrophic host cell. After several gene transfer events, about 95 % of the genetic information was handed over from the chloroplast to the nuclear genome. Therefore, nuclear-encoded chloroplast proteins that are synthesized in the cytosol need to be imported into the chloroplast. Protein import into chloroplasts is a highly regulated process, which requires fine-tuning mechanisms especially during chloroplast differentiation. In addition to the transit peptide, efficient targeting of these proteins require additional assistance from several cytosolic players. Most notably, preproteins harbor features to bind the heat shock chaperone proteins HSP70 and HSP90. Furthermore, a subset of proteins also bind to 14-3-3. Together with HSP70, 14-3-3 dimer binds to preproteins forming together a so-called “guidance complex”. Formation of these complexes enhances the import rate of the preproteins. The phosphorylation of preproteins at the transit peptide increases the affinity of 14-3-3, hence, enhancing import efficiency. In *Arabidopsis thaliana*, three high homologous cytosolic serine/threonine/tyrosine (STY) protein kinases are responsible for the phosphorylation of preproteins: STY8, STY17 and STY46.

In first part of this work, I investigated the role of precursor phosphorylation and kinase regulation in acclimating conditions. We could show that high light acclimation enhances the phosphorylation yield of several precursors and kinase expression. We also show that heat treatments has detrimental effects on precursor phosphorylation yield and kinase expression. STY8, STY17 and STY46 harbor a conserved ACT domain upstream of the kinase domain. The ACT domain is a widely distributed structural motif, known to be important for the allosteric regulation of many enzymes. In the second part of this work, I investigated the role of the ACT domain in the regulation of the STY kinase *in vivo* and *in vitro*. Here we could show that the ACT domain regulates autophosphorylation as well as substrate phosphorylation of the STY kinases *in vitro*. We identified Ile and s-adenosylmethionine as binding partners of the ACT domain, negatively influencing its autophosphorylation ability. Moreover, we investigated the role of the ACT domain *in planta* and could confirm its involvement in chloroplast differentiation *in vivo*.

Zusammenfassung

Chloroplasten entstanden in Folge eines endosymbiontischen Ereignisses, bei dem ein photosynthetisches Cyanobakterium von einer heterotrophen Wirtszelle aufgenommen wurde. Durch mehrmaligen Gentransfer wurden ca. 95% der genetischen Information aus dem Chloroplasten in das Kerngenom übertragen. Daher müssen nuklear-kodierte Chloroplastenproteine, die im Zytosol synthetisiert werden, in den Chloroplasten importiert werden. Proteinimport in den Chloroplasten ist ein stark regulierter Transportprozess, der insbesondere bei der Differenzierung von Chloroplasten Regulationsmaßnahmen erfordert. Außer dem Transitpeptid benötigen Präproteine zusätzliche zytosolische Akteure um ein effizientes Targeting zu gewährleisten. Präproteine können von Chaperonen, den Hitzeschock-Proteinen HSP70 und HSP90, gebunden werden. Darüber hinaus bindet eine Teilgruppe von Proteinen auch an 14-3-3 Dimere. Präproteingebundene 14-3-3-Dimere formen zusammen mit HSP70 einen sogenannten „Guidance-komplex“. Die Bildung dieser Komplexe erhöht die Importrate der Präproteine. Die Phosphorylierung des Transitpeptids eines Präproteins erhöht die Affinität von Präproteinen zu 14-3-3 Dimeren und damit auch die Importeffizienz. In *Arabidopsis thaliana* wurden drei homologe zytosolische Serin/Threonin/Tyrosin (STY) - Proteinkinasen identifiziert, die chloroplastidäre Präproteine phosphorylieren: STY8, STY17 und STY46.

In dem ersten Teil der vorliegenden Arbeit wurden die Bedeutung und Funktionsweise der Präproteinphosphorylierung und Kinaseregulierung unter akklimativen Umweltbedingungen untersucht. Es konnte gezeigt werden, dass bei hoher Lichtintensität die Phosphorylierung einiger Präproteine und die Kinaseexpression erhöht sind. Ich konnte auch zeigen, dass Wärmebehandlungen einen negativen Effekt auf den Grad der Phosphorylierung der Präproteine und Kinaseexpression erzeugen. STY8, STY17 und STY46 besitzen eine konservierte ACT-Domäne, die im N-terminalen Bereich des Proteins liegt. Die ACT-Domäne ist ein weit verbreitetes Strukturmotiv das häufig in Enzymen vorkommt, wobei sie deren Aktivität allosterisch reguliert. Im zweiten Teil dieser Arbeit wurde die Rolle der ACT-Domäne bei der Regulation der STY-Kinase *in vivo* und *in vitro* untersucht. Hier konnten wir *in vitro* zeigen, dass die ACT-Domäne sowohl die Autophosphorylierung der STY-Kinasen als auch die Präproteinphosphorylierung reguliert. Des Weiteren wurden Isoleucin und s-Adenosylmethionin als Bindungspartner der ACT-Domäne identifiziert. Beide Metabolite haben eine negative Auswirkung auf die Autophosphorylierung der STY-Kinasen und Präproteinphosphorylierung. Schlussendlich habe ich die Rolle der ACT-Domäne *in planta* untersucht, wodurch eine Funktion bei der Chloroplastendifferenzierung gezeigt werden konnte.

Abbreviations

³² P	Radioactive Phosphorus-32
Ala	Alanine
ACT	Aspartate kinase, Chorismate mutase and TyrA
Arg	Arginine
Asn	Asparagine
Asp	Aspartatic Acid
At	Arabidopsis thaliana
ATP	Adenosine-5'-triphosphate
BLAST	Basic local alignment search tool
bp	Basepair
CAB1	Chlorophyll a-b binding protein 1
Col-0	Columbia ecotype 0
CBB	Coomassie brilliant blue
Cys	Cysteine
DNA	Deoxyribonucleic acid
dNTPs	Deoxynucleotide triphosphate
cDNA	Copy-DNA
Clp2	CLP Protease Proteolytic subunit 2
C-terminus	Carboxyl-terminus
DTT	Dithiothreitol
E.coli	Escherichia coli
ECL	Enhanced chemiluminescence
EDTA	Ethylenediaminetetraacetic acid
EGTA	Ethylene glycol-bis(β-aminoethyl ether)-N,N,N',N'-tetraacetic acid
gDNA	Genomic DNA
GFP	Green fluorescence protein
Gln	Glutamine
Glu	Glutamic Acid
Gly	Glycine
HCF101	High chlorophyll fluorescence 101
His	Histidine
Ile	Isoleucine
IPTG	Isopropyl β-D-1-thiogalactopyranoside
LB	Lysogeny broth
Leu	Leucine
Lys	Lysine
kDa	Kilo Dalton
KD	Dissociation constant
Met	Methionine
MgCl	Magnesium Chloride
MST	Microscale Thermophoresis
MW	Molecular weight
NdhM	M subunit of NAD(P)H:plastoquinone dehydrogenase complex
N-terminus	Amino-terminus
NaCl	Sodium Chloride

OD	Optical density
OE23	Oxygen evolving complex protein of 23 kDa
PAGE	Polyacrylamide gel electrophoresis
Phe	Phenylalanine
PCR	Polymerase chain reaction
Pro	Proline
RFP	Red fluorescence protein
PVDF	Polyvinylidene difluoride membrane
RNA	Tibonucleic acid
RNAi	RNA interference
Rpm	Revolutions per minute
RT-PCR	Reverse transcriptase PCR
RT-qPCR	Real-time quantitative PCR
Ser	Serine
SSU	Ribulose-1,5-bisphosphate carboxylase/oxygenase, small subunit
SAM	S-Adenosyl methionine
T-DNA	Transfer DNA
Thr	Threonine
TEMED	Tetramethylethylenediamine
Tic	Translocon at the inner envelope of chloroplasts
Toc	Translocon at the outer envelope of chloroplasts
Trp	Tryptophan
Tyr	Tyrosine
Val	Valine
WT	Wild type

1. Introduction

1.1 Preprotein Import into Chloroplast

Chloroplasts are distinct organelles that arose during endosymbiosis 1.5 billion years ago. Here, the ancestral photosynthetic cyanobacterium was engulfed by a heterotrophic host eukaryote containing mitochondria (Gould et al., 2008). Subsequently, 95% of the genetic material coding for approximately 3000 proteins was transferred from the chloroplast to the nuclear genome. Therefore, nuclear encoded chloroplast proteins have to be translocated to the chloroplast upon their synthesis in the cytosol. In order for proper targeting to occur, the protein requires the presence of transit sequences at the N-terminus of the newly synthesized proteins. The N-terminal sequence is then cleaved after import to the organelle (reviewed in Bruce, 2000; Leister, 2003). As a first step of the import process, the preprotein interacts with receptors located at the outer envelope membrane of the chloroplast. Then, in an energy dependent manner, these proteins are transported through the outer and inner envelopes. Through-out the import process, the chloroplast-targeted preproteins interact with the two multi-protein translocon complexes Toc (translocon at the outer membrane of chloroplast) and Tic (translocon at the inner membrane of chloroplast). This process is known as the “general import pathway” (reviewed by Schwenkert et al., 2011; Sjuts et al., 2017). An alternative import pathway has also been described in detail, but the general import pathway is believed to be the primary preprotein import route into chloroplast (see review by Sjuts, et al., 2017). The import process commences with the recognition of the preprotein by the Toc receptors: Toc159 and Toc34/33. Both are integral membrane GTPases exposed largely at the cytosol (Kessler & Schnell, 2006). Toc159 consists of three functional domains: an intrinsically disordered acidic domain (A-domain), the GTPase domain (G-domain) and the membrane anchor domain (M-Domain with a mass of ~54 kDa) (Bolter et al., 1998; Chen et al., 2000; Richardson et al., 2014). Both proteins are anchored at the outer envelope membrane via their C-termini. In a GTP dependent manner, the preprotein first binds to Toc159 and then are relayed to Toc34 (see Andres et al., 2010 for review). It has also been proposed that Toc34 may also act as an initial receptor (Kessler & Schnell, 2009). The preprotein is then transferred to Toc75, the translocation channel of the chloroplast outer membrane and final member of the Toc core complex (Hinnah et al., 1997). Structurally, Toc75 is a β -barrel-type integral membrane channel protein. It has been shown *in vitro*, using lipid vesicles, that the three Toc proteins are sufficient for the translocation of preproteins in lipid vesicles (see review Schleiff & Soll, 2003). Studies in peas revealed that the multiprotein complex has a 1:4:4 of Toc159/Toc34/Toc75 stoichiometric distribution ratio (Schleiff et al., 2003). A further Toc component was identified which was found in the vicinity of the Toc core complex, named Toc64. However, this protein has been shown to play a less

significant role in chloroplast protein import (Andres, et al., 2010). Toc64 displays its C-terminal domain to the cytosol while being anchored to the outer membrane of the chloroplast. Furthermore, the C-terminal domain is composed of three tetratricopeptide motifs (TPR) mandatory for protein-protein interaction. Interestingly, there are studies suggesting its possible involvement in preprotein recognition by functioning as an initial docking station for HSP90-bound preproteins which are then delivered to Toc34 (Qbadou et al., 2006). An additional feature of the Toc64 protein is that it extends into the intermembrane space connecting it with the so-called intermembrane space (IMS) translocation complex. Despite limited characterizations in the proteins localized in this complex, the general consensus is that it mediates the preprotein translocation from the Toc to the Tic translocons (Schnell et al., 1997). To date, two components have been identified: Tic22 and IMS HSP70.. Tic22 transiently interacts with the inner envelope membrane. A linker-type functionality has been suggested to facilitate preproteins transport between the Toc and Tic translocation complexes (review by Schwenkert, et al., 2011; Sjuts, et al., 2017). Upon crossing the IMS, the preproteins encounter components of the Tic complex in the inner envelope, the final stage of preprotein import. As of yet, this complex comprises eight components (see Kovacs-Bogdan et al., 2010 for review). Tic22 is the only soluble unit of this complex. The most abundant component of the Tic translocon is Tic110, which forms the main import pore on the inner envelope membrane. Tic20 is the second channel-like component of the Tic complex. This component has been suggested to translocate a specific class of preproteins (Kikuchi et al., 2009). However, the consensus still remains that Tic110 is the foremost prime channel of the Tic translocon. Tic40 is anchored via its N-terminal domain to the inner envelope membrane. Its C-terminal domain is exposed to the stromal side, which allows protein-protein interaction to take place with Tic110 and the ATPase chaperone HSP93. HSP93, in an ATP dependent manner, processes the unfolding of preproteins, and hence with Tic40, form the “motor complex” for import. Tic62, Tic55 and Tic32, which formulate the ‘redox-regulon’ are responsible for the redox regulation of the import process. Tic62 and Tic32 are membrane proteins that interact with Tic110 in a specific redox state in the stroma. Tic55 is anchored to the inner envelope membrane via its C-terminal domain. The molecular function of Tic55 remains unclear. However, recently a study was published in which a hydroxylation activity during leaf-senescence-dependent chlorophyll breakdown was demonstrated for Tic55 (Hauenstein et al., 2016). There has been suggestion that Tic62, Tic32 and Tic55 to mediate preprotein import is due to their possessions of specific domains: NADP(H)-binding site for Tic62 and Tic32 and a Rieske-type iron-sulphur centre for Tic55 (see Balsera et al., 2009 for review). However, single knockout mutants do not have significant effect in protein import (Bolter et al., 2015). The import of chloroplast precursor proteins across the outer and inner membrane concludes with the cleavage of the transit

peptide by a metallo-peptidase called stroma processing peptidase in the stroma before the mature proteins are properly folded and assembled (see Paetzel et al., 2002 for review).

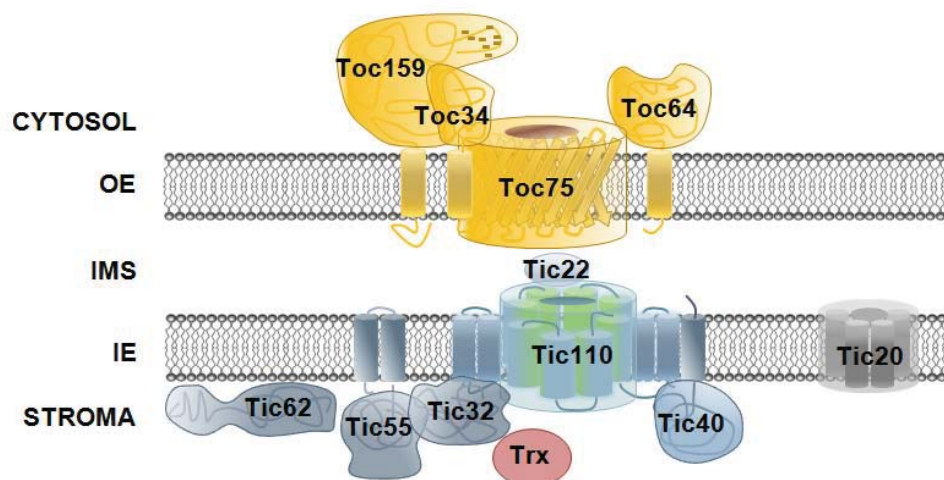


Figure 1: Model of the preprotein import into the chloroplast. Nuclear encoded chloroplast proteins are translocated across the outer (OE) and inner envelope (IE) of the chloroplast via the Toc and Tic translocons. After translocation, the transit peptide is cleaved and the mature protein can fulfill its function in the stroma. (Schwenkert and Bölder 2016)

1.2 Targeting to the Chloroplast

Recent studies have elaborately elucidated the transport process of chloroplast precursor proteins via the general import pathway. However, their targeting mechanism still requires further exploration. The consensus so far is that nuclear-encoded chloroplast proteins interact with heat shock chaperone protein HSP70. HSP70, a 70 kDa protein, facilitates proper folding of proteins in an ATP-dependent manner (see review by Mayer & Bukau, 2005). Despite having been shown to bind to both transit peptide and mature sections of chloroplast preproteins, HSP70 binding shows a higher affinity to the chloroplast transit peptide (see review by Zhang & Glaser, 2002). In addition to HSP70, chloroplast precursors have also been shown to interact with two further cytosolic chaperones: the chaperone HSP90 (Qbadou, et al., 2006) and a 14-3-3 dimer (May & Soll, 2000). *In vitro* analysis revealed that each chaperone binds to a specific subset of chloroplast preproteins (Fellerer et al., 2011). Binding to HSP90 is predicted to repress aggregation of unfolded preproteins in the cytosol while escorting the proteins to the Toc64 docking site (Qbadou et al., 2007). Precursor binding to 14-3-3 offers an alternative import route. 14-3-3, a small (~ 30 kDa) acidic protein, dimerizes and binds to a large number of different substrates involved in a plethora of cellular processes in eukaryotic cells (Bridges & Moorhead, 2005; Dougherty & Morrison, 2004). Therefore, it has been predicted that preprotein binding to both HSP70 and 14-3-3 after synthesis (forming so-called “guidance complex”) ensures reduced aggregation and enhanced import rate (May & Soll, 2000). In addition, it has been shown that

phosphorylation of precursor enhances its binding affinity to 14-3-3 and, hence, promotes guidance complex formation. The phosphorylation state of the precursor has been shown to positively alter the 14-3-3 binding motifs (May & Soll, 2000). Chloroplast presequences consist of a variety of different amino acids, but the overall charge still remains positive. Together, with the predominance of serine and threonine residues which have been recently shown to often lie within 14-3-3 binding motifs, it ensures the phosphorylation process to be reversible (May & Soll, 2000; Waegemann & Soll, 1996). However, lack of phosphorylation does not render the precursor import incompetent or lead to mistargeting (Nakrieko et al., 2004). Nevertheless, it has been shown to enhance precursor affinity to Toc34 (Schleiff et al., 2002). Interestingly, it has also been shown that dephosphorylation of chloroplast preproteins affects protein import (Waegemann & Soll, 1996). Nevertheless, most of these studies have been performed *in vitro* and, hence, may not reflect the importance of phosphorylation depending on different stages of plant development or environmental conditions. The physiological relevance of these studies causes contention regarding its importance. In *Arabidopsis thaliana*, it has been shown that cytosolic protein kinases STY8, STY17 and STY46 play a role the transit peptides phosphorylation (Martin et al., 2006).

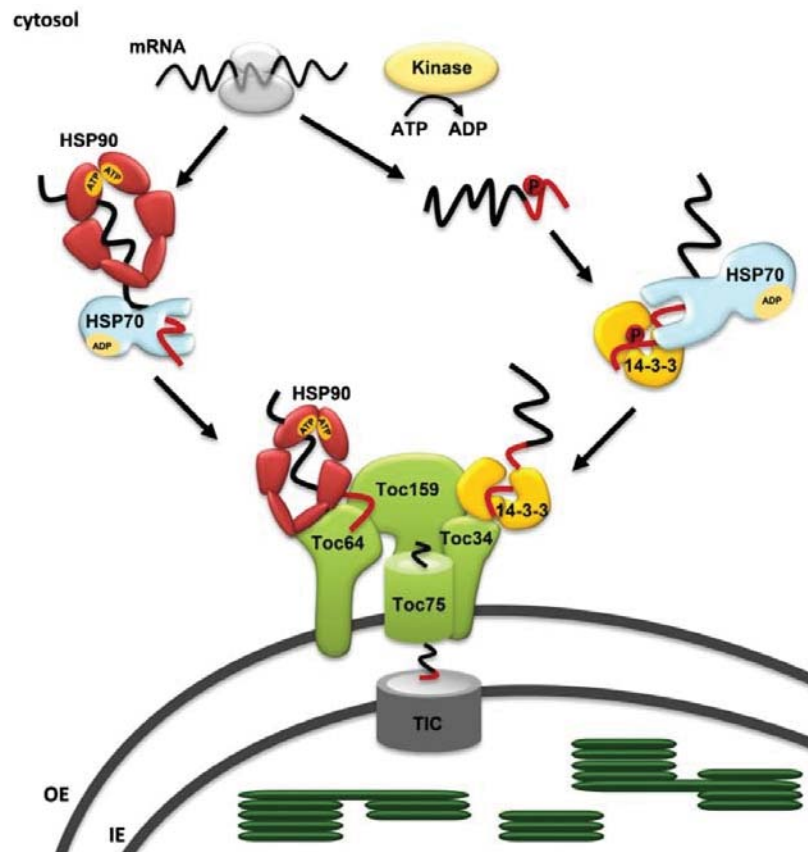


Figure 2. Cytosolic components of the import pathway. Precursors, which are synthesized in the cytosol are recognized by HSP70, HSP90 or 14-3-3 proteins, respectively. 14-3-3 binding precursors are initially phosphorylated by a specific kinase and further guided to Toc34. In contrast HSP90-bound precursors use Toc64 as a first docking station, from where they are passed on to Toc34 and Toc75 (Schwenkert et al. 2011).

1.3 Plant Protein Kinases

Protein kinases are phospho-transferases that modify proteins, by chemically adding phosphate groups to a specific residue (phosphorylation). Specifically, the process involves the transfer of the γ -phosphate from an ATP donor molecule to a serine, threonine or tyrosine hydroxyl group on the protein substrate. As in all signaling processes, the phosphorylation of proteins occurs as a result of a response to specific stimuli. Stimuli types range from extracellular messenger molecules, environmental signals, and endogenous stimuli. As a consequence, target proteins are either switched on/off (see review by Hunter, 1987). Therefore, protein phosphorylation is central to many regulatory pathways in plants despite only 3.2% of the genome encodes for protein kinases. (see Krupa et al., 2006 for review).

1.4 Plant Dual Specificity Kinases

It has been commonly observed that protein kinases are classified as serine/threonine kinases and tyrosine kinases (Hanks et al., 1988). An abundance of evidence displays that

serine/threonine phosphorylation mediates the regulation of many cellular processes, both in animals and plants. The significance of tyrosine phosphorylation has not been extensively shown in plants in comparison to animals. Therefore, no further exploration of such kinases took place until the discovery of protein tyrosine phosphatases in *Arabidopsis thaliana* (see Luan, 2002 for review). As time progressed, mass spectrometry based searches have advanced to demonstrate that tyrosine phosphorylation does indeed take place in plants (de la Fuente van Bentem & Hirt, 2009). Despite changes in perception, plant-specific tyrosine kinases were still not identified. The discovery of plant specific dual specific protein kinases that phosphorylate both serine/threonine and tyrosine has been suggested to overcome this discrepancy. Such proteins has been found to be present in many types of higher plants such as rice, soybean, tomato, wheat, barley, alfalfa, beech and *Arabidopsis thaliana* (see Rudrabhatla et al., 2006 for review). These plant specific dual kinases were coined as STY kinases.

1.5 *Arabidopsis thaliana* STY Kinases

Using a BLAST search against the consensus protein tyrosine kinase motif CW(X)6RPXF, 57 *Arabidopsis thaliana* protein kinases have been identified to be distributed among all five chromosomes (see Rudrabhatla, et al., 2006 for review). Furthermore, in-depth analysis of the kinase catalytic domains showed 11 conserved sub-domains. Alongside the consensus protein tyrosine kinase motif CW(X)6RPXF in the sub-domain XI, the catalytic domain of all the 57 kinases also present the KXXN motif in sub-domain VI suggesting targeting towards specific serine and threonine residues (Rudrabhatla, et al., 2006). These highly homologous cytosolic proteins have other highly conserved functional regions aside from the protein tyrosine catalytic domain. The kinase catalytic domain contains similar characteristics to other know kinase catalytic domains consisting of a small and a large lobe, which are essential to bind ATP, coordination, substrate recognition, and catalysis. Data obtained from microarrays show various expression profiles spreading throughout tissues and developmental stages. Hence, it is strongly suggested that these kinases play a role in different plant cellular processes (Rudrabhatla, et al., 2006). Furthermore, these proteins can be sub-divided into four groups which include members of many different protein kinase classes. Group I is further divided into four families: the ANT-like kinases, the peanut STY-related kinases, the soybean GmPK6-like kinases and the ATMRK-like kinases. Group II mainly consists of MAP3K/CTR1/EDR1 protein kinases and is further divided in three families: the PB1 domain/GmPK6/EDR1/MAPK3 like kinases, the PAS domain/MAP3K/CTR1/EDR1-like kinases and the MAP3K/CTR1/EDR1-like kinases. Group III consists of protein kinases containing ankyrin domain repeat motifs and group IV includes light sensory kinases related to *Ceratodon purpureus* phytochrome kinases (Rudrabhatla, et al., 2006). Interestingly, the kinases of group I, precisely the ANT-like kinases, the peanut

STY-related kinases and the soybean GmPK6-like kinases, have the tyrosine consensus sequence RWMAPE in the subdomain VIII in addition to the one in subdomain XI, suggesting that these kinases are evolutionarily more closer to the protein tyrosine kinase family (LambertiGugel et al., 2011). In addition, it has been shown that peanut STY-related kinase STY13 is actually able to phosphorylate tyrosine beside serine/threonine residues (Reddy & Rajasekharan, 2007; Rudrabhatla, et al., 2006). Other three members of the peanut STY-related kinase family include: STY8, STY17 and STY46.

1.6 STY8, STY17, and STY46

Recently, *in vitro*, it has been shown that STY8, STY17 and STY46 can phosphorylate chloroplast transit peptides at serine and threonine, but not tyrosine residues (Lamberti, et al., 2011; Martin, et al., 2006). It has been argued that its ability of phosphorylating tyrosine residues is lost as a result of evolution. In addition, deletion of these proteins revealed a delay in the greening process, inefficient chloroplast differentiation, and reduction of nucleus-encoded chloroplast proteins, hence, supporting a role of cytosolic STY kinases in chloroplast differentiation (Lamberti, et al., 2011). Therefore, it has been proposed that these kinase might play a role in cytosolic phosphorylation of precursors at transit peptides before import into chloroplast. How the STY kinases are regulated in stress conditions or environmental changes still requires investigation. Interestingly, upstream of the kinase domain of these proteins is a conserved ACT domain. *In vitro* data shows that deletion of this domain, causes not only hyperphosphorylation of the kinase but also the precursor when incubated simultaneously. Therefore, the ACT domain might play a regulatory role in kinase activity *in vivo*.

1.7 The ACT Domain

The term ACT domain was derived from the first letters of three proteins, aspartate kinase-chorismate mutase-tyrA (prephenate dehydrogenase). The ACT domain is a structural motif found in proteins with various functions such as control of metabolism, solute transport, and signal transduction (Chipman & Shaanan, 2001; Grant, 2006; Lang et al., 2014). The amino acids sequence of the ACT domain ranges from 75 and 80 amino acids. The prototypical ACT domain is comprised of four β strands and two α helices organized in a $\beta\alpha\beta\beta\alpha\beta$ fold formation. The structural motif was suggested as a result of PSI-Blast (position-specific iterating-Blast) sequence data base search using the small subunit (IlvN) of acetolactate synthase. Subsequently, a plethora of proteins containing the ACT domain were found to be involved in amino acid and purine metabolism and were found to be regulated by specific amino acids (Chipman & Shaanan, 2001). A subset of transcriptional regulators have specific ACT domains that bind to transcription factors. These specific types of ACT domains was named RAM domain (Regulator of Amino acid Metabolism)(Chipman & Shaanan, 2001;

Grant, 2006; Lang, et al., 2014). Mutagenesis and crystallization of more proteins containing ACT domain added in-depth information regarding the secondary structure elements of the ACT domains. Therefore, when adopting the pattern of secondary structure, similarities between the RAM domain and ACT domain were observed.

1.8 ACT domain Sequence Homology and Structure

Using the “protein family data base” (Pfam), 3779 proteins have been identified in Bacteria, Archaea, and Eukaryotes, including vertebrates, plants, fungi, and single cellular organisms that contain an ACT domain. However, advanced sequence alignment methods were utilized to detect the proteins containing the ACT domain. This speaks to the lack of conservation found within the ACT domains. Remarkably, a conserved glycine residue was identified in the turns between alpha helices and beta sheets (Grant, 2006). This was predicted to be the ligand binding site in all ACT domains. Interestingly, the conserved glycine residues in the RAM domains were rather primarily found between the loops of two beta sheets (Grant, 2006). Until now, at least 10 ACT domain-containing protein structures have been determined. Of these, five have been solved with bound ligand. The structure differences range from stand-alone ACT domains, as seen for the YbeD protein from *E. coli*, to large multimeric proteins with ACT domains either isolated or associating into groups of 2, 3, or 4. The prototypical domain display a two side-by-side domains forming an extended beta sheet. This has been observed *E. coli* phosphoglycerate dehydrogenase, aspartate kinase from *Arabidopsis*, and the *E. coli* llvH regulatory subunit of acetohydroxyacid synthase, to name a few (Grant, 2006).

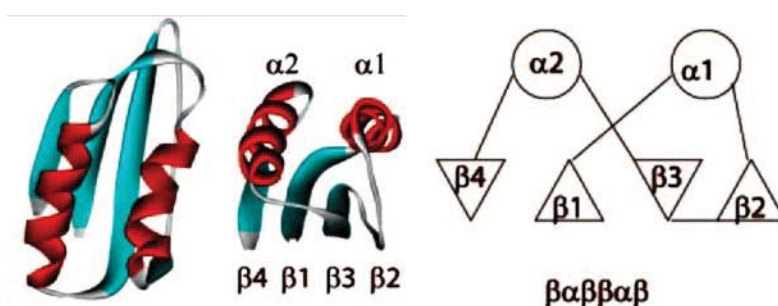


Figure 3: ACT domain. A single ACT domain from *E. coli* D-3-phosphoglycerate dehydrogenase displaying the $\beta\alpha\beta\beta\alpha\beta$ motif. In the diagram, the triangles point up or down to indicate the direction of the strand in the β sheet. Numbers progress from N terminus to C terminus (Grant 2006).

1.9 ACT Domain Ligand Binding Sites and Mechanism

To date, there are four different ligand binding motifs found in ACT domains (Chipman & Shaanan, 2001; Grant, 2006; Lang, et al., 2014). According to the five structures that have been characterized, the consensus observed was that ligands tend to bind at the interfaces between ACT domains which display the extended 8-stranded β sheet structure. Furthermore, the glycine residues located in loops between the helices and sheets seems to play a significant role in the ligand-domain interaction. For example, the glycine residues between $\alpha 1$ and $\beta 1$ in the ACT domain of phosphoglycerate dehydrogenase and aspartate kinase seem to play a role in the binding to L-serine and L-lysine, respectively (Mas-Droux et al., 2006; Thompson et al., 2005). A second binding motif is observed in the ATP-phosphoribosyltransferase. This protein does not contain any glycine residues. Its substrate (L-histidine), associates mainly with the loop between the $\alpha 1$ helix and $\beta 2$ strand (Cho et al., 2003; Lohkamp et al., 2004). The third ligand binding motif is observed in the YkoF structure (Devedjiev et al., 2004). This protein contains two polypeptide chains that each contain two consecutive ACT domains. Hence, when both chains associate, they form a dimer and, consequently, binds to four ligands. Interestingly, only one of the chains contain glycine residue in the loop between the ACT domains. The second chain does not contain any glycine residue but does not seem to disrupt the ligand binding capabilities of the domains (Devedjiev et al., 2004). The fourth and final binding motif is observed in the NikR transcription regulator (Schreiter et al., 2003). Here, a nickel ion binds at the loop between $\beta 2$ and $\beta 3$. Subsequently, the nickel interacts with the side chain of a histidine residue. It has been shown that some enzyme activity is inhibited upon ligand binding. This is observed in *E. coli* D-3-phosphoglycerate dehydrogenase (Thompson et al., 2005). Here, binding to its ligand (serine), causes the disruption of the of the substrate binding domain. Contrastingly, phenylalanine stabilizes phenylalanine hydroxylase upon substrate binding (Mitnaul & Shiman, 1995). Furthermore, histidine synergistically enhances the inhibition of ATP-phosphoribosyltransferase by AMP and ADP. Therefore, the histidine stabilizes the hexamer and hence partially closes the active site. The ACT domain generally seems to play a role on regulating the enzymatic activity of enzymes (Chipman & Shaanan, 2001; Grant, 2006; Lang, et al., 2014).

2. Materials & Methods

2.1. Materials

2.1.1. Chemicals

All used chemicals were purchased in high purity from Sigma-Aldrich (Steinheim, Germany), Fluka (Buchs, CH), Roth (Karlsruhe, Germany), Roche (Penzberg, Germany), Merck (Darmstadt, Germany), AppliChem (Darmstadt, Germany) or Serva (Heidelberg, Germany).

2.1.1. Molecular Weight Markers and DNA Standards

For agarose gel electrophoresis, *EcoRI* and *HindIII* digested λ -Phage DNA (MBI Fermentas) was used as a molecular size marker. For SDS-PAGE, peqGOLD protein marker I (VWR, Ismaning, Germany) was used. Amersham HMW Calibration Kit for Native Electrophoresis (GE Healthcare, Munich, Germany) was used for Native-PAGE.

2.1.2. Oligonucleotides

DNA oligonucleotids were ordered from Metabion (Martinsried, Germany) and are listed below.

Oligonucleotide	5'-3' oligonucleotide sequence	Purpose
STY8_Sacl_fr	AGTGAGCTCATGACGATCAAAGAT	cloning pET21a ⁺
STY8_NotI_rev	TGCTTAGCGGCCGCCACTACGACGTTTAC	cloning pET21a ⁺
STY8_attb_fr	GGGGACAAGTTTGTACAAAAAAGCAGGCTTAATGACGATCAAAG ATGAG	cloning in pDONOR207
STY8_attb_rev	GGGGACCACTTTGTACAAGAAAGCTGGGTACACTACGACGTTT ACCTC	cloning in pDONOR207
STY8 Δ ACT_fr	TTGTCTACACGACCGAAGCTTAAGGATCAA	deletion of ACT domain
STY8 Δ ACT_rev	TTGATCCTTAAGCTTCGGTCGTGTAGACAA	deletion of ACT domain
STY17_Sacl_fr	AGTGAGCTCATGGCGATCAAAGAG	cloning pET21a ⁺
STY17_NotI_rev	TGCTTAGCGGCCGCACGATGGCCTTTTTT	cloning pET21a ⁺
STY17_attb_fr	GGGGACAAGTTTGTACAAAAAAGCAGGCTTAATGGCGATCAAA GAGGAG	cloning in pDONOR207
STY17_attb_rev	GGGGACCACTTTGTACAAGAAAGCTGGGTAACGATGGCCTTTTT TTAG	cloning in pDONOR207
STY17 Δ ACT_fr	CCTAATTCTCGACCGAAGTTTAAGGATCAA	deletion of ACT domain
STY17 Δ ACT_rev	TTGATCCTTAACTTCGGTCGAGAATTAGG	deletion of ACT domain
STY46_Sacl_fr	AGTGAGCTCATGGTGATGGAGGAC	cloning pET21a ⁺
STY46_NotI_rev	TGCTTAGCGGCCGCATGATGTGTGGTGCT	cloning pET21a ⁺
STY46_attb_fr	GGGGACAAGTTTGTACAAAAAAGCAGGCTTAATGGTGATGGAG GACAAC	cloning in pDONOR207

STY46_attb_rev	GGGGACCACTTTGTACAAGAAAGCTGGGTAATGATGTGTGGTG CTTCT	cloning in pDONOR207
STY46 Δ ACT_fr	CTCTATTCACGGCCCAAGATCGAGTTGCAG	deletion of ACT domain
STY46 Δ ACT_rev	CTGCAACTCGATCTTGGGCCGTGAATAGAG	deletion of ACT domain
ACT_fr_Sacl	agtcGAGCTCATGCACGAGATCACTTT	cloning pET21a ⁺
ACT_rev_NotI	CCCACCGCGGCCGCCAGTATTTCTTTGCTCA	cloning p pET21a ⁺
pOE23_Sacl_fr	agtcGAGCTCATGGCGTACAGTGCGTGT	cloning pET21a ⁺
pOE23_NotI_rev	CCCACCGCGGCCGCAGCAACACTGAAAGAAGT	cloning pET21a ⁺
pHCF101_Sacl_fr	agtcGAGCTCATGCCGCTTCTTCATCCACA	cloning pET21a ⁺
pHCF101_NotI_rev	CCCACCGCGGCCGCGACTTCGACTGGAGACAA	cloning pET21a ⁺
pPetC_Sacl_fr	agtcGAGCTCATGGCGTCTCATCC	cloning pET21a ⁺
pPetC_NotI_rev	CCCACCGCGGCCGCAGACCACCATGGAGC	cloning pET21a ⁺
pPORA_Sacl_fr	agtcGAGCTCATGGCCCTTCAAGCT	cloning pET21a ⁺
pPORA_NotI_rev	CCCACCGCGGCCGCGCCAAGCCCACGAG	cloning pET21a ⁺
pClp2_Sacl_fr	agtcGAGCTCATGGCGGTCTCGTTTAAT	cloning pET21a ⁺
pClp2_NotI_rev	CCCACCGCGGCCGCGCCTAGCCCTGCGCTTTC	cloning pET21a ⁺
pNdhM_Sacl_fr	AGTGAGCTCATGGTTGCAGCATTC	cloning pET21a ⁺
pNdhM_NotI_rev	TGCTTAGCGGCCGCAGCGTCTCTTGAGG	cloning pET21a ⁺
pFNRL1_Sacl_fr:	agtcGAGCTCATGGCTGCTGCTATA	cloning pET21a ⁺
pFNRL1_Sacl_fr:	CCCACCGCGGCCGCGTAGACTTCAACATT	cloning pET21a ⁺
STY8QRT-PCR for	CCACGGATGGAAGTATGAGT	quantitative RT-PCR
STY8QRT-PCR rev	TACACGATCAGGCTTGAGAAA	quantitative RT-PCR
STY17QRT-PCR for	AAGGTTTAAA AGATGCATTG A	quantitative RT-PCR
STY17QRT-PCR rev	CATCAGTTCCATCCGTAGGTA	quantitative RT-PCR
STY46QRT-PCR for	AGGTGCCAGA ACGCATGTTC C	quantitative RT-PCR
STY46QRT-PCR rev	TTGATAGCAACTTCCTGGCTA	quantitative RT-PCR
RUB1_qpcr_fr	CTGTTACGGAACCCAATTC	quantitative RT-PCR
RUB1_qpcr_rev	GGAAAAAGGTCTGACCGACA	quantitative RT-PCR

2.1.2. Plasmids

Gene	Organism	Vector	Description	Source	Purpose
STY8	Arabidopsis	pET21a ⁺	C-terminal His-tag	This Work	expression in <i>E. coli</i>
STY8 Δ ACT	Arabidopsis	pET21a ⁺	C-terminal His-tag	This Work	expression in <i>E. coli</i>
STY8 T439A	Arabidopsis	pET21a ⁺	C-terminal His-tag	This Work	expression in <i>E. coli</i>
STY8 G197D	Arabidopsis	pET21a ⁺	C-terminal His-	This Work	expression in

			tag		E.coli
STY17	Arabidopsis	pET21a ⁺	C-terminal His-tag	This Work	expression in E.coli
STY17 Δ ACT	Arabidopsis	pET21a ⁺	C-terminal His-tag	This Work	expression in E.coli
STY46	Arabidopsis	pET21a ⁺	C-terminal His-tag	This Work	expression in E.coli
STY46 Δ ACT	Arabidopsis	pET21a ⁺	C-terminal His-tag	This Work	expression in E.coli
ACT-STY8	Arabidopsis	pET21a ⁺	C-terminal His-tag	This Work	expression in E.coli
pOE23	Arabidopsis	pET21a ⁺	C-terminal His-tag	This Work	expression in E.coli
pClp2	Arabidopsis	pET21a ⁺	C-terminal His-tag	This Work	expression in E.coli
pHCF101	Arabidopsis	pET21a ⁺	C-terminal His-tag	This Work	expression in E.coli
pPETC	Arabidopsis	pET21a ⁺	C-terminal His-tag	This Work	expression in E.coli
pNdhM	Arabidopsis	pET21a ⁺	C-terminal His-tag	This Work	expression in E.coli
pPORA	Arabidopsis	pET21a ⁺	C-terminal His-tag	This Work	expression in E.coli
pFNRL1	Arabidopsis	pET21a ⁺	C-terminal His-tag	This Work	expression in E.coli
STY8	Arabidopsis	pK7WGF2	C-terminal GFP-tag	This Work	expression in plant
STY8	Arabidopsis	pH2GW7	No tag	This Work	expression in plant
STY8 Δ ACT	Arabidopsis	pK7WGF2	C-terminal GFP-tag	This Work	expression in plant
STY8 Δ ACT	Arabidopsis	pH2GW7	No tag	This Work	expression in plant
STY17	Arabidopsis	pK7WGF2	C-terminal GFP-tag	This Work	expression in plant
STY17 Δ ACT	Arabidopsis	pK7WGF2	C-terminal GFP-tag	This Work	expression in plant
STY46	Arabidopsis	pK7WGF2	C-terminal GFP-tag	This Work	expression in plant
STY46	Arabidopsis	pB7WGF2	C-terminal GFP-tag	This Work	expression in plant
STY46 Δ ACT	Arabidopsis	pK7WGF2	C-terminal GFP-tag	This Work	expression in plant
STY46 Δ ACT	Arabidopsis	pB7WGF2	C-terminal GFP-tag	This Work	expression in plant

pSSU	Tobacco	pET21d	C-terminal His-tag	Prof. Jürgen Soll Laboratory	expression in E.coli
mSSU	Tobacco	pET21d	C-terminal His-tag	Prof. Jürgen Soll Laboratory	expression in E.coli
tLhcb2.2-mSSU	Arabidopsis/Tabak	pET21d	C-terminal His-tag	Prof. Jürgen Soll Laboratory	expression in E.coli

2.1.3. Antibodies

Antibody	Clonality	Species	Immunoblot	Source
anti-STY8	polyclonal	Rabbit	1:500	Prof. Jürgen Soll Laboratory
anti-STY17	polyclonal	Rabbit	1:500	Prof. Jürgen Soll Laboratory

2.1.4. Kits

All the kits were used according to the manufacturer instructions.

Kits	Purpose	Source
QIAprep Spin Miniprep Kit	Plasmid DNA isolation	Qiagen
QIAGEN Plasmid Midi Kit	Plasmid DNA isolation	Quiagen
NucleoSpin Extract II	Purification of DNA	Quiagen
iScript™ cDNA Synthesis Kit	cDNA synthesis	Bio-Rad
Rneasy Plant Mini Kit	RNA extraction from Plant	Quiagen
FastStart DNA Master SYBR-Green Plus kit	Quantitative RT-PCR	Roche
LR clonase II Enzyme Mix	In Vitro Gateway cloning System	Invitrogen
BP clonase II Enzyme Mix	In Vitro Gateway cloning System	Invitrogen
Wheat germ lysate translation kit	In Vitro translation	Promega
Reticulocyte lysate translation kit	In Vitro translation	Promega
L007 Monolith NT.115 protein labelling kit RED-tris-NTA	Microscale Thermophoresis	Nanotemper

2.1.5. Enzymes

Enzymes purchased was used according to the manufacturer instructions.

Enzymes	Source
---------	--------

Restriction Enzymes	New England BioLabs (NEB)
T4 DNA Ligase	New England BioLabs (NEB)
TAQ DNA Polymerase	New England BioLabs (NEB)
Phusion DNA Polymerase	New England BioLabs (NEB)
Shrimp Alkaline Phosphatase (rSAP)	New England BioLabs (NEB)
Lambda Protein Phosphatase (Lambda PP)	New England BioLabs (NEB)
Cellulase Onozuka R10	Serva
Macrozym R10	Yakult Honsha
Rnase-free Dnase I	Amersham Bioscience

2.1.6. Protein Purification Column

Ni Sepharose 6 Fast Flow and were purchased from GE Healthcare.

2.1.7. Software

MultAlin – Multiple sequence alignment by Florence Corpet (INRA Toulouse, France) was used to align DNA and protein sequences The universal protein resource (UniProt) was used to predict targeting peptides. To process microscale thermophoresis (MST) data and to generate binding affinity values, Nanotemper MO.Affinity Analysis software was used. For secondary structure predictions JPred4 online software by Geoffrey J Barton (University of Dundee) was used.

2.1.8. Bacterial Strains

Bacterial strains	Organism	Genotype
TOP10	<i>E. coli</i>	F- mcrA Δ (mrr-hsdRMS-mcrBC) ϕ 80lacZ Δ M15 Δ lacX74 nupG recA1 araD139 Δ (ara-leu)7697 galE15 galK16 rpsL(StrR) endA1 λ
RIPL (BL21-CodonPlus(DE3)-RIPLE strain)	<i>E. coli</i>	<i>E. coli</i> B F- ompT hsdS(rB- mB-) dcm+ Tetr gal λ (DE3) endA Hte [argU proLCamr] [argU ileY leuW Strep/Specr]
AGL-1 (Lazo et al. 1991)	<i>Agrobacterium tumefaciens</i>	AGL0 recA::bla pTiBo542 Δ T Mop+CbR
GV3101 (pMP90RK)(Koncz and Schell, 1986)	<i>Agrobacterium tumefaciens</i>	C58C1 pMK90RK, Rifr, Gmr, Kmr

2.1.9. Plants

WT *Arabidopsis thaliana* seeds of the ecotype Columbia (Col-0) were obtained from Lehle Seeds (Round Rock, USA). The *sty8 sty46* and *sty8 sty46 sty17-14* mutants has been described elsewhere (Lamberti, et al., 2011). WT, *sty8 sty46* and *sty8 sty46 sty17-14* seeds

were obtained from plants grown on soil. Seeds of *Nicotiana benthamiana* were used for the growth of tobacco plants.

2.2. Methods

Standard methods were performed as described by Sambrook and Russell, 2001.

2.2.1. Cloning

Vector	Type	Cloning System
pET21a ⁺	Restriction Enzyme	pET Cloning System
pET21d ⁺	Restriction Enzyme	pET Cloning System
pDONR207	Entry	Gateway Cloning System
pK7FWG2	Destination	Gateway Cloning System
pB7FWG2	Destination	Gateway Cloning System
pH2GW7	Destination	Gateway Cloning System

2.2.1.1. Restriction enzyme cloning

PCR fragments were amplified using appropriate oligonucleotide pairs of oligonucleotides and a template DNA from plasmid or from cDNA obtained from *Arabidopsis thaliana*. PCR conditions were adjusted according to the size of the fragment of interest. For protein overexpression, expression vector pET21a⁺ was utilized. Appropriate oligonucleotides were designed to generate fragments with sticky ends. Gel electrophoresis was performed and the DNA fragment was extracted using NucleoSpin Extract II. The fragment purified and the vector were digested using appropriate restriction endonucleases. Following vector digestion, the vector was dephosphorylated using Shrimp Alkaline Phosphatase (rSAP). Following all enzyme reactions, both fragments and vector were purified using NucleoSpin Extract II. Ligation of fragment and vector was performed using T4 DNA Ligase. The ligation product was chemically transformed in competent *E.coli* TOP10 cells and plated on LB plates with the appropriate antibiotic. Single colonies were inoculated in liquid culture, let grown over night and the plasmid DNA was purified using the QIAprep Spin Miniprep Kit (QIAGEN). The DNA insert was fully sequenced.

2.2.1.2. Gateway System Cloning

Appropriate oligonucleotides with attB attachment sites were generated. PCR was performed to generate DNA Fragments with flanking attachment sites. The DNA with extraction sites were purified using Gel electrophoresis followed by NucleoSpin Extract II. Constructs were cloned via homologous recombination from pDONR207 into binary destination vectors. Cloning was performed according to the manufacturer's instructions.

2.2.1.3. Sequencing

Each fragment or plasmid was confirmed by sequencing which was performed by the sequencing service of the Faculty of Biology (Ludwig-Maximilians-Universität München, Germany) using 100 -200 ng of DNA with appropriate oligonucleotides. The sequence obtained was aligned against the sequence of interest using online multiple sequence alignment tool Multalin.

2.2.2. Transformation of *A. tumefacium*

1 - 2 µg plasmid was added to GV3101 or AGL1 cells for stable transformation of *A. thaliana* or transient expression of *N. benthamiana*, respectively. Cells were incubated 5 min on ice then 5 min in liquid nitrogen. Heat shock was performed for 5 min at 37 °C then 800 µl LB were added and cells were incubated shaking for 4 h at 28 °C before plated on LB plates with appropriate antibiotics. Cells were grown for 2- 3 days at 28 °C.

2.2.3. Bacterial Growth Conditions

E. coli was cultivated in LB medium (1 % peptone from casein, 0.5 % yeast extract, 171 mM NaCl) at 37°C in either liquid culture or on agar-plates supplemented with the appropriate antibiotics according to the resistance (Ampicillin 100 µg/ml, Kanamycin 50 µg/ml and Spectinomycin 50 µg/ml). *Agrobacterium tumefaciens* was cultivated in LB medium at 28°C in either liquid culture or on agar-plates supplemented with the appropriate antibiotics according to the resistance (Carbenicillin 100 µg/ml, Kanamycin 25 µg/ml, Spectinomycin 100 µg/ml, 40 µg/ml Gentamicin and 100 µg/ml Rifampicin).

2.2.4. Plant Growth Conditions

Arabidopsis thaliana WT Columbia ecotype (Col-0) and the respective mutants were grown either on soil or on half-strength MS (Murashige and Skoog) medium supplemented with 1% sucrose under controlled conditions in a growth chamber. For phenotyping analysis plants were grown on soil in long day condition (16h/8h light/dark, 22°C, 120 µE m For greening experiments dry seeds were surface-sterilized and vernalized at 4°C for 2 days. Petri dishes were exposed to light (120 µE) for 6 h and were then placed in the dark. After 6 days in the dark, petri dishes were exposed to light for the indicated period of time.

2.2.5. Overexpression and purification of recombinant soluble proteins from *E.coli*

E. coli bacteria was transformed and cultivated in at 37 °C to an OD₆₀₀ of 0.6 - 0.8. Overproduction was induced by the addition of 1 mM isopropyl β-D-1-thiogalactopyranoside (IPTG) and incubated for 16 h at 14 °C. After elapsed time, the culture was centrifuged for 15 min at 3000 g. The supernatant was discarded and resuspended in lysis buffer (20 mM Tris

pH 7.5, 200 mM NaCl). After cell fractionation using microfluidizer (Microfluidics, Westwood, USA), the sample was centrifuged at 18000 rpm 4 °C for 30 min and the supernatant was rotated with 250 µl Ni Sepharose at 4 °C for 1 h. The beads were washed three times with 5 ml wash buffer (20 mM Tris pH 7.5, 200 mM NaCl, 10 mM imidazole). Subsequently, the recombinant proteins was eluted with increasing concentration of imidazole (50mM to 500 mM imidazole). For quality control, fractions were analysed using SDS-PAGE.

2.2.6. Purification of proteins out of inclusion bodies from *E.coli*

After the subsequent centrifugation after cell fractionation, the pellet was washed one time with 20 ml detergent buffer (20 mM Tris pH 7.5, 200 mM NaCl, 1 % deoxycholic acid, 1 % nonidet P-40, 10 mM β-mercaptoethanol), twice with Triton buffer (20 mM Tris pH7.5, 0.5% Triton X-100, 5 mM β-mercaptoethanol), and finally two times with Tris buffer (20 mM Tris pH 8.0, 10 mM DTT). Centrifugation was performed at 12000 rpm, 4 °C for 10 min. Finally, the pellet was resuspended in 5 ml urea buffer (50 mM Tris pH 8.0, 100 mM NaCl, 7 M urea) and rotated for up to 12 h at room temperature. After centrifugation at 20000 rpm, room temperature for 15 min, the supernatant was rotated with 250 µl Ni Sepharose at room temperature for 2 h (50 mM Tris pH 8.0, 100 mM NaCl, 7 M urea). Subsequently, the recombinant proteins were eluted with increasing concentration of imidazole (50 mM to 500 mM imidazole). For quality control, fractions were analysed using SDS-PAGE.

2.2.7. Isolation of proteins from *A. thaliana*

A. thaliana leaves were homogenized in homogenization medium (50 mM Tris pH 8.0, 10 mM EDTA, 2 mM EGTA, 10 mM DTT) using liquid nitrogen and electronic micropestle manually. The powdered suspension was incubated for 10 min at room temperature in the dark and centrifuged at 10000 rpm, 4 °C for 10 min. Supernatant contained soluble proteins, pellet resuspended in homogenization medium contained membrane proteins.

2.2.8. Determination of protein concentration

Concentration of proteins was determined using Bradford reagent (0.1 % Coomassie brilliant blue G-250, 5 % ethanol, 10 % phosphoric acid). 1 µl protein sample was mixed with 1:5 diluted Bradford reagent and absorption was measured against buffer at 595 nm.

2.2.9. Relative molecular mass estimation by size exclusion chromatography

A superdex 200 increase 3.2/300 grade size exclusion chromatography column (GE Healthcare) was equilibrated with buffer (50 mM Tris-HCl, 150 mM NaCl, pH 7.4). The column was calibrated using gel filtration standards (Thyroglobulin, M_r 669,000: void volume; Ferritin, M_r 440,000; Aldolase, M_r 158,000; Canalbumin, M_r 75,000; Ovalbumin M_r 44,000. 20

µl of concentrated protein at 1 mg/mL was applied to the equilibrated column and eluted using the above buffer. The relative molecular masses of the peaks obtained were calculated using a logarithmic interpolation.

2.2.10. Microscale Thermophoresis

MST assays were carried out with a Monolith NT.115 instrument according to instruction manual (Nano Temper, Munich, Germany). Briefly, 100 µl of 100 nM of purified His-tag protein was mixed with 100 µl of 50 nM of L007 Monolith NT.115 protein labelling kit RED-tris-NTA dye for 30 min in a total volume of 200 µl. Increasing concentrations (from 25nM to 1mM range) of non-labelled ligand were titrated against a final concentration of 25 nM His-tagged protein. Finally, the mixture was soaked into hydrophilic silicon capillaries (K004 Monolith NT.115). Each measurement was performed three times. Experiments were carried out in 50 mM Tris, pH 7.4, 150 mM NaCl, 10 MgCl₂, 0.05% (w/v) Tween 20. Data evaluation was performed with the Monolith software.

2.2.11. SDS polyacrylamide gel electrophoresis (SDS-PAGE)

Protein separation was performed by SDS-PAGE discontinuous gels (Laemmli, 1970). The gel consists of a stacking gel (5 % polyacrylamide) and a running gel (10 - 15 %polyacrylamide). Samples were loaded with SDS loading buffer (62.5 mM Tris pH 6.8, 2 %SDS, 10 % glycerol, 5 % β-mercaptoethanol, 0.004 % bromphenol blue). Gels were run inSDS running buffer (25 mM Tris, 192 mM glycine, 0.1 % SDS) and subsequently either stained with Coomassie (45 % methanol, 9 % acetic acid, 0.2 % Coomassie brilliant blue R-250) or used for western blotting.

2.2.12. Non-denaturing gradient gel electrophoresis (Native-PAGE)

A modified method described Hough et al., 1987 was used to prepare 5-10% gradient PAGE gel was described in Hames (1998). Gels were ran with NativeMarker™ protein marker (Life Technoloies, Carisbad, CA). Samples were loaded with loading buffer (62.5 mM Tris pH 6.8, 2 %, 10 % glycerol, 0.004 % bromphenol blue, and 0.5 % Coomassie brilliant blue G-250). Gels were run in running buffer (25 mM Tris, 192 mM glycine) and subsequently stained with Coomassie (45 % methanol, 9 % acetic acid, 0.2 % Coomassie brilliant blue G-250).

2.2.13. Semi-dry electro blot and immunodetection of proteins

After protein separation using SDS gels, the gel was blotted onto a PVDF membrane (from Macherey-Nagel (Düren, Germany) using a semi-dry blotting apparatus. Blotting conditions were adjusted according to gel size and thickness. Blots were assembled as follows on the anode: three blotting papers from Millipore (Darmstadt, Germany) in anode I buffer (20 % methanol, 300 mM Tris), two blotting papers in anode II buffer (20 %

methanol, 25 mM Tris), activated membrane, gel, three blotting papers in cathode buffer (20 % methanol, 40 mM aminocaproic acid). Transfer was carried out for 1.5 h at 0.8 mA/cm. The membrane was stained briefly with ponceau solution (5 % acetic acid, 0.3 % ponceau) and washed with TBST (20 mM Tris pH 7.6, 137 mM NaCl, 0.075 % Tween). For immunodetection of proteins, membrane was blocked for 1 h with 5 % skimmed milk in TBST. After three times washing for 10 min, the membrane was incubated with primary antibody over night at 4 °C. After two times 15 min washing in TBST, the membrane was incubated for 2 h at room temperature with horse radish peroxidase conjugated secondary antibody. After three times 10 min washing in TBST membrane was incubated in equal volumes of development solution I (100 mM Tris pH 8.5, 1 % luminol, 0.44 % coomarcic acid) and II (100 mM Tris pH 8.5, 0.018 % H₂O₂) and signal was detected with enhanced chemiluminescence using Image Quant LAS 400 (GE Healthcare).

2.2.14. Phosphorylation Assay

Assays were performed as described in Lamberti et al., 2011. Briefly, 1 µg recombinant substrate protein was incubated with 0.5 µg recombinant kinase in the present of 13.5 µCi gamma ³²P-ATP (Hartmann Analytic, Braunschweig, Germany) in a total volume of 25 µl kinase buffer (20 mM Tris/HCl pH 7.5, 5 mM MgCl₂, 0.5 mM MnCl₂). The reaction was performed 20 min at room temperature and stopped by the addition of 7 µl 4x SDS sample buffer. Proteins were separated by SDS-PAGE, dried, and phosphorylation signals were detected by phosphor plate imaging.

2.2.15. Detection of radiolabeled proteins

Dried SDS gels are exposed overnight to BAS-MS phosphor imaging plates (FUJIFILM) which are analyzed using a Typhoon scanner (GE healthcare).

2.2.16. *Arabidopsis thaliana* stable transformation with *Agrobacterium tumefaciens*

The construct of interest was transformed in *Agrobacterium tumefaciens* (GV3101) and plated on LB plates with appropriate antibiotics for selection. A single colony was inoculated in LB media with appropriate antibiotics and incubated at 28 °C until OD₆₀₀=0.8 was achieved. Cells were centrifuged 15 min at 3500 rpm and pellet was resuspended in a Silvet-medium (5 % sucrose, 0.05 % silvet L-77) to final OD₆₀₀ of 0.8. *Arabidopsis thaliana* plants already showing primary and secondary bolts were transformed by floral dip (Clough & Bent, 1998). Seeds obtained from the transformed plants were selected on MS plates supplemented with the appropriate antibiotic (25 µg/ml Hygromycin or 15 µg/ml BASTA).

2.2.17. Isolation of genomic DNA from *Arabidopsis thaliana*

A single *Arabidopsis* leaf was cut and transferred to a 1.5 ml microtube containing 200 µl of extraction buffer (200 mM Tris-HCl (pH 7.5), 250 mM NaCl, 0.5% SDS). The sample was homogenized using a polytron with a pestle. Afterwards, the homogenate was incubated at room temperature (RT) for 3-5 min and then centrifuged at 13000 x g for 10 min. 150 µl of the supernatant were transferred to a new tube. To precipitate the genomic DNA, 150 µl of isopropanol was added to the tube, carefully mixed and centrifuged at 13000 x g for 15 min at 4°C. The pellet was subsequently air-dried and finally resuspended in 50 µl of distilled water.

2.2.18. Quantitative RT-PCR analysis

RNA was isolated from plants using the Plant RNeasy extraction kit (Qiagen) according to instruction manual. The RNA isolated was treated with DNase and, subsequently, cDNA was synthesized by reverse transcription (*iScript* Reverse Transcriptase Bio-Rad). For quantitative RT-PCR the FastStar DNA Master SYBR-Green Plus kit was used and the reaction was performed in a CFX96 Touch Real-Time PCR Detection System (Bio-Rad) using the appropriate pairs of oligonucleotides. The relative abundance of all transcripts amplified was normalized to the expression level of housekeeping gene for RUB1 (Related To Ubiquitin 1) conjugating enzyme 1, RCE1. The RCE1 gene was used as an internal reference in other studies (Romani et al., 2015; Voigt et al., 2010). Data was extracted using Bio-Rad CFX Manager (Bio-Rad) and evaluated using Microsoft Excel (Microsoft).

2.2.19. Transient transformation and protoplast isolation of *Nicotiana benthamiana*

3 to 4 week old single *Nicotiana benthamiana* grown on soil were used for transient transformation. *Agrobacterium tumefaciens* (AGL1) carrying the construct of interest was grown in LB medium until OD₆₀₀ =0.8 was achieved. Cells were centrifuged 15 min at 4000 rpm and resuspended in a Agromix Agromix (10 mM MgCl₂, 10 mM MES/KOH pH 5.6, 150 µM Acetosyringone) to achieve OD =1. The resuspension was 2 h in the dark at 23°C and the bacterial solution was infiltrated using 1 ml syringe at the lower site of the *Nicotiana benthamiana* leaf. The infiltrated *Nicotiana benthamiana* plants were watered and put in dark 2-3 days. After elapsed time, two leaves were cut incubated with 1 % Cellulase R10 and 0.3 % Macerozyme R10 in 10 ml F-PIN medium (MS medium PC-vitamins (200 mg/l Myoinositol, 1 mg/l thiamin-HCl, 2 mg/l Ca-panthotenate, 2 mg/l nicotinic acid, 2 mg/l pyridoxin-HCl, 0.02 mg/l biotin), 1 mg/l 6-benzylaminopurin (BAP), 0.1 mg/l a-naphthaleneacetic acid (NAA), 20 mM MES, pH 5.8 (KOH), 80 g/l glucose, Osm 550) for 2 h.

The resulting suspension was carefully filtered through a gauze using a cut pipette tips. 2 ml F-PCN medium (F-PIN, except instead of glucose, sucrose was added as the osmoticum) was overlayed on the filtered suspension and centrifuged for 10 minutes at 70 x g. The intact protoplasts were collected from the interface between the F-PIN and F-PCN media, washed with W5 buffer and GFP fluorescence was observed with a TCS-SP5 confocal laser scanning microscope (Leica, Wetzlar, Germany).

2.2.20. Chlorophyll Extraction

Chlorophyll content measurement of Arabidopsis leaves was performed according to method described by (Porra et al., 1989). Approximately 150 mg of total leaf tissue was harvested and incubated in 2 ml of dimethylformamide for 2 h in the dark. Absorbance was measured at 663, 750, and 645 nm. Chlorophyll concentration was calculated as described (Arnon, 1949)

3. Results

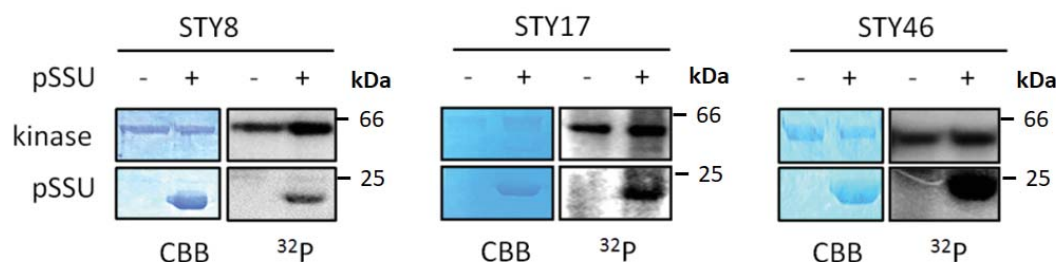
3.1. Effects of Acclimation on STY kinases

It has been shown that varying degrees of light intensities and temperature impact the expression of several chloroplast genes (Niyogi, 1999; Pfalz et al., 2012; Rossel et al., 2002). However, the underlying mechanisms responsible for plant acclimation to abiotic factors are poorly understood. Nonetheless, due to the advancement of microarray studies, several nuclear encoded genes have been identified to play a role in the initial acclimation-sensing pathways (Richmond & Somerville, 2000; Schenk et al., 2000). There has been extensive studies linking temperature stress to photosynthesis (reviewed in Mathur et al., 2014). Despite significant advancement in the temperature-acclimation studies in terms of chloroplast protein import, light-acclimated studies on other hand have been few.

3.1.1. STY kinases phosphorylates nuclear encoded chloroplast precursors that associates with 14-3-3 and HSP70 chaperones

To investigate the enzymatic properties of the STY kinases, full-length of *STY8* (At2g17700), *STY17* (At4g35708), and *STY46* (At4g38470) cDNAs were cloned into a pET21a⁺ vector, expressed in *E. coli*, and purified via a C-terminal His tag on Ni²⁺-Sepharose. Kinase phosphorylation was investigated in the purified sample by radioactive labeling in presence and absence of the preprotein pSSU. Our data shows kinase autophosphorylation and precursor phosphorylation activity (Figure 4A). To identify new phosphorylation targets of the STY kinases, we selected precursors that have been shown to interact with 14-3-3 and HSP70 (Fellerer, et al., 2011). We selected several proteins, cloned the respective genes into pET21a⁺, over expressed, and purified the proteins from *E. coli* via a C-terminal His-tag and subjected them to an *in vitro* kinase assay using recombinant STY8. The preprotein of pSSU, which is phosphorylated (Waegemann & Soll, 1996) in the transit peptide *in vitro*, was used as a positive control model substrate. All proteins but mSSU, which was used as a nonphosphorylatable control, were found to be phosphorylated (Figure 4B).

A)



B)

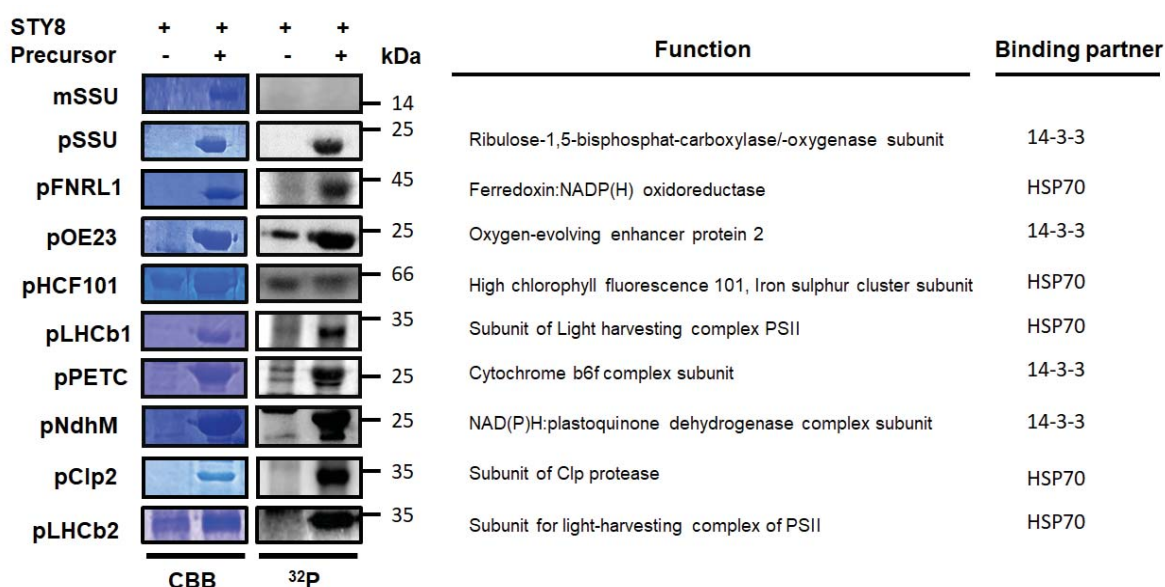


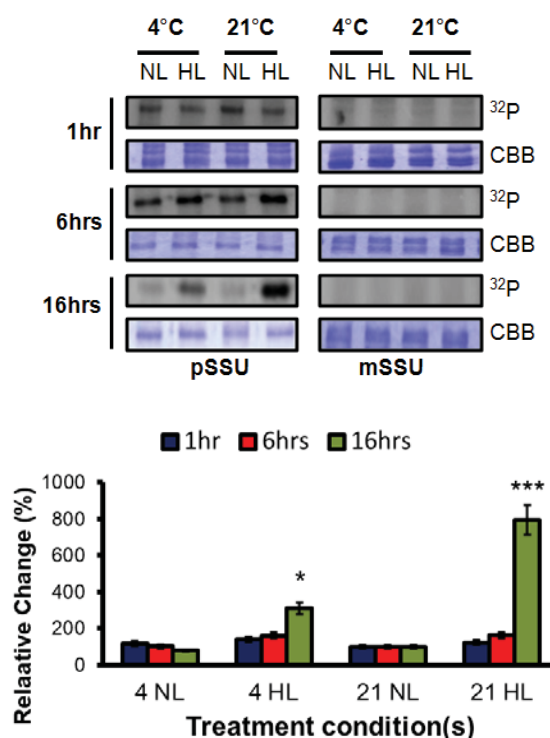
Figure 4: STY kinases phosphorylate nuclear encoded chloroplast precursors.

A) 1 μg *E. coli* purified STY8, STY17, and STY46 were subjected to an *in vitro* kinase assay in presence and absence of *E. coli* purified pSSU for 10 min, and phosphorylation was detected by autoradiography, showing autophosphorylation activity and phosphorylation of pSSU. Coomassie blue staining (CBB) gel is also shown. B) 2 μg of *E. coli* purified nuclear-encoded precursors of pSSU, ferredoxin-NADP(+)-oxidoreductase (pFNRL1), oxygen-evolving complex 23 (pOE23), high chlorophyll fluorescence 101 (pHCF101), chlorophyll a-b binding protein 1 (LHCb1), chloroplast cytochrome B6/F complex Rieske iron-sulfur protein subunit (pPETC), chloroplast NADH Plastoguinone Dehydrogenase complex M (pNdhM), *Clp* protease subunit 2 (pCLP2), and Chlorophyll a-b binding protein 2.1 (pLHCb2) were subjected to an *in vitro* kinase assay with 1 μg *E. coli* purified STY8. Mature subunit of Rubisco (mSSU) was used as a negative control. Phosphorylation was detected by autoradiography. Coomassie blue staining (CBB) gel is also shown. All blots were repeated at least three times ($n=3$).

3.1.2. High light affects precursor phosphorylation yield

In order to investigate the effect of light intensity and/or temperature on the phosphorylation of precursors, we exposed 14 days-old wild-type *A. thaliana* plants to 1 hr, 6 h, and 16 h to low (4°C) and standard (21°C) temperatures in combination with either normal light (100 $\mu\text{mol photons m}^{-2} \text{s}^{-1}$) or high light (500 $\mu\text{mol photons m}^{-2} \text{s}^{-1}$). Subsequently, soluble proteins from leaves were extracted and used to conduct an *in vitro* kinase assay. We observed a significant change in precursor phosphorylation yield when plants were exposed to high light for 16 h (Figure 5A). In addition, combination with low temperature yielded reduced precursor phosphorylation yield when compared to standard temperature. To investigate whether the effect is also observed in pFNRL1, pOE23, pHCF101, LHCb1, pPETC, pNdhM, pCLP2, pLHCb2, we repeated the high light experiments using different precursors. Indeed, we observe increase in phosphorylation yield in all precursors (Figure 5B). Our result shows that light intensity is the more important denominator to affect precursor phosphorylation yield *in vitro*.

A)



B)

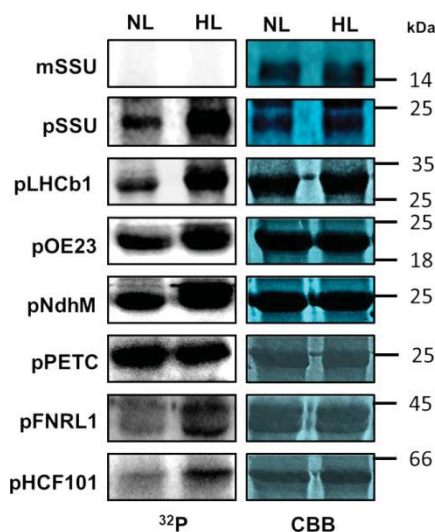
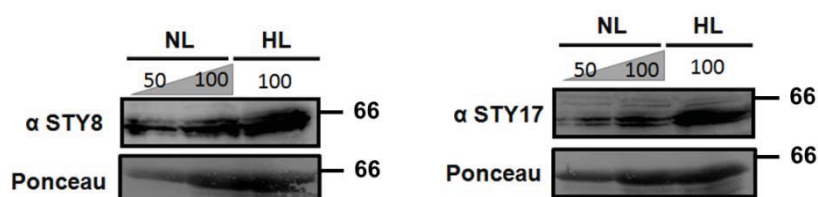


Figure 5: High light acclimated-plants increase precursor phosphorylation yield. A) Kinase assay showing phosphorylation yield of pSSU in WT under high light and cold. 14-day-old wild-type was treated at high light ($500 \mu\text{mol photons m}^{-2} \text{s}^{-1}$) and/or cold (4°C). Total soluble protein extracts were prepared and incubated with radioactive [γ - ^{32}P]-ATP and pSSU as substrate. All assays were repeated at least three times ($n=3$). Representative pictures are shown in and relative pSSU phosphorylation yield quantified by ImageJ is shown below. Data show the mean \pm s.e.m.; $n = 3$. Statistical significance was determined by a Student t-test. A P value <0.05 was considered statistically significant compared to untreated control. Asterisks indicate statistical significance. B) Kinase assay showing phosphorylation yield of precursors pSSU, pLHCb1, pOE23, pNdhM, pPETC, pFNRL1, and pHCF101 in WT under normal light and high light. 21-day-old wild-type was treated at high light ($500 \mu\text{mol photons m}^{-2} \text{s}^{-1}$). Total soluble protein extracts were prepared and incubated with radioactive [γ - ^{32}P]-ATP and several precursors as substrate. After 10 min incubation, phosphorylation was detected by autoradiography. Coomassie blue staining (CBB) gel is also shown.

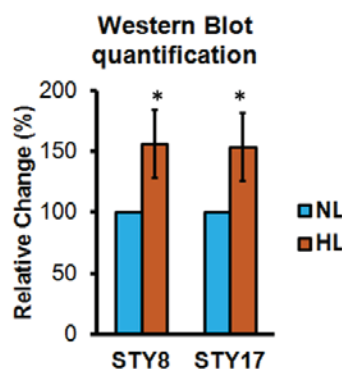
3.1.3. Kinase expression is upregulated in high light acclimation

Upon observing increase of precursor phosphorylation levels in high light conditions, we examined the expression levels of STY8, STY17, and STY46 (Figure 3). Analyses of the protein level with specific STY8 and STY17 antisera show an increase of 25% of normal light protein levels (Figure 6A and 6B). Unfortunately, no antibody for STY46 was available. To evaluate kinase transcript expression levels, we performed quantitative RT-PCR with RNA isolated from wild-type plants exposed to 16 h of high light. Our results indicated upregulation of all the kinases. Most significant upregulation was observed in STY46 with almost five-fold increase in expression followed by STY8 and STY17 (both at approximately three fold) (Figure 6C).

A)



B)



C)

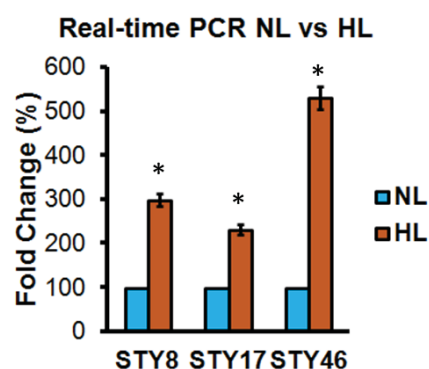


Figure 6: Kinase expressions are upregulated in high light acclimating conditions. A) 14-day-old wild-type plants grown on soil were treated with high-light for 16 h. Total extracted soluble proteins were prepared and separated on SDS–PAGE gel and probed with anti-STY8 or anti-STY17. B) Quantification of immunoblotting was performed with ImageJ software (National Institute of Health). All immunoblots were repeated at least three times. Data show the mean \pm s.e.m.; $n = 3$. Statistical significance was determined by Students t-test. A P value <0.05 was considered statistically significant compared to untreated control. Asterisks indicate statistical significance. C) Quantitative RT-PCR was performed with STY8, STY17, and STY46 to analyze the expression level ($n = 3$). RUB1-conjugating enzyme, RCE1, was used as a housekeeping gene.

3.1.4. Double mutant shows reduced precursor phosphorylation yield

To confirm kinase involvement in precursor phosphorylation in normal light and high light acclimated conditions, double mutants of *sty8 sty46*, and *sty8 sty46/35S::STY46* complementation lines were obtained (Lamberti, et al., 2011). The *STY46* cDNA was sufficient to completely restore the wild-type phenotype in comparison to *STY8* cDNA. For our acclimation studies, we treated WT, double mutant, and complementated plants for 16 h normal light ($100 \mu\text{mol photons m}^{-2} \text{s}^{-1}$) or high light ($500 \mu\text{mol photons m}^{-2} \text{s}^{-1}$). Total soluble protein extracts were isolated and incubated with radioactive $[\gamma\text{-}^{32}\text{P}]\text{-ATP}$ and pSSU as substrate. Our results show that the double mutant showed reduced precursor phosphorylation levels compared to WT independent of light treatment (Figure 7). The complementation line showed similar levels to WT in both normal light and high light

conditions. These findings indicate that the kinases enhance precursor phosphorylation independent of light conditions.

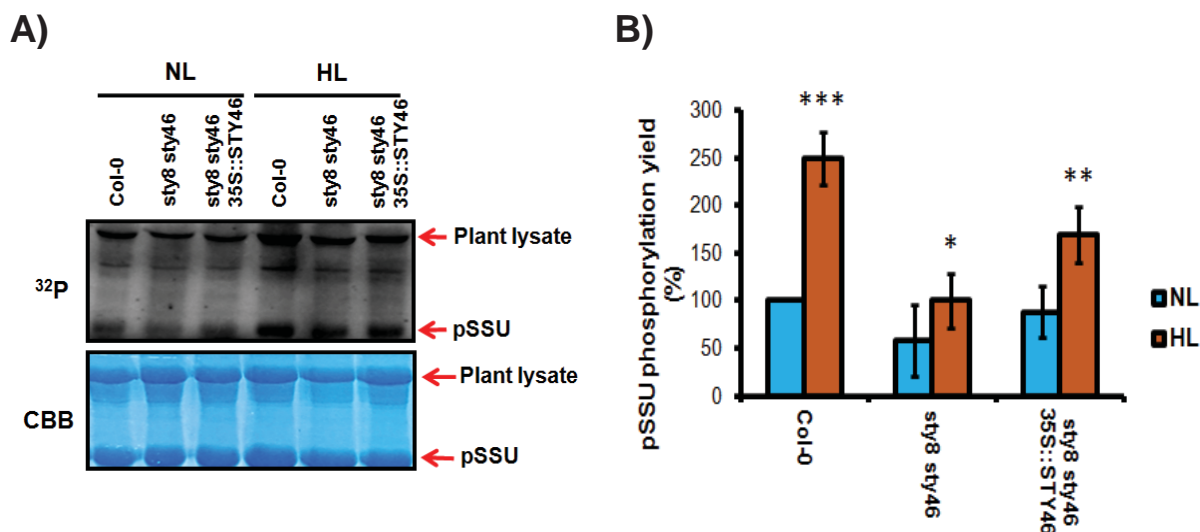
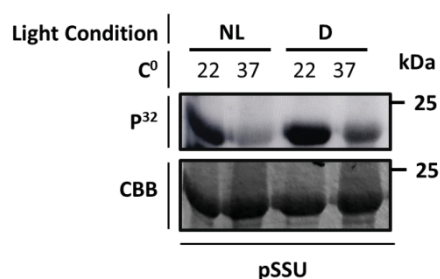


Figure 7: Double mutant shows reduced precursor phosphorylation yield. Kinase assay of phosphorylation yield of pSSU in WT, *sty8 sty46* mutant and complementation under high light. 14-day-old wild-type, *sty8 sty46*, and *sty8 sty46/35S::STY46* complementation were treated at high light for 16 h. Total soluble protein extracts were prepared and incubated with radioactive [γ -³²P]ATP and pSSU as substrate. Representative pictures are shown in (A), and relative pSSU phosphorylation yield is shown in (B). All assays were repeated at least three times (n=3). Data show the mean \pm s.e.m. Statistical significance was determined by Students t-test. A P value <0.05 was considered statistically significant compared to untreated control. Asterisks indicate statistical significance.

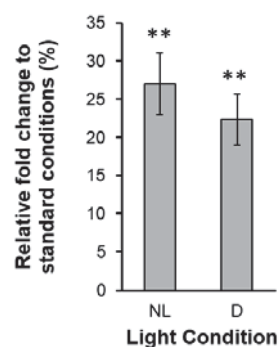
3.1.5. Precursor phosphorylation and kinase expression is downregulated in heat acclimation

In order to investigate the effect of heat and or dark acclimation on the phosphorylation of precursors *in vitro*, we exposed 14 days-old wild-type plants to normal light or dark conditions at 22°C or 37°C for 1 h. Subsequently, soluble proteins from leaves were extracted and used to conduct an *in vitro* kinase assay in presence of pSSU. We observed a significant reduction in precursor phosphorylation yield at heat acclimation irrespective to the light conditions (both five-fold). To evaluate the kinase expression in such conditions, we used the same soluble extract and conducted a western blot with STY8 and and STY17 specific antibodies. Indeed, we did observe a significant reduction in both kinase expressions. Our result shows that plant exposure to short term heat, significantly hampers precursor phosphorylation *in vitro* (Figure 8).

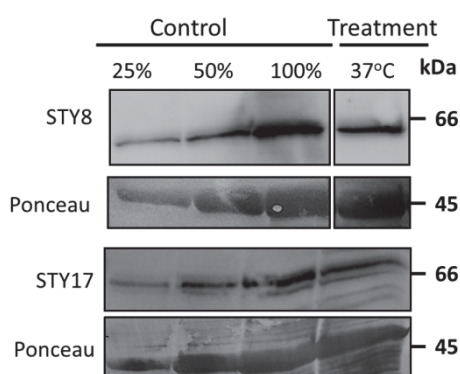
A)



B)



C)



D)

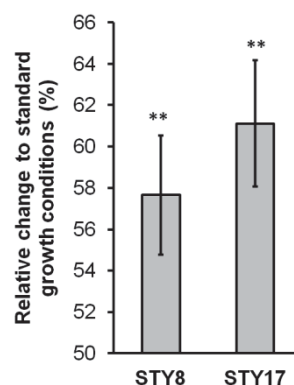


Figure 8: Precursor phosphorylation and kinase expression is down regulated in heat acclimation. A) Kinase assay of phosphorylation yield of pSSU in WT, *sty8 sty46* mutant and complementation under high light. 14-day-old wild-type were treated at normal light or dark conditions 22°C or 37°C for 1 h. Total soluble protein extracts were prepared and incubated with radioactive [γ - ^{32}P]-ATP and pSSU as substrate. C) 14-day-old wild-type plants grown on soil were treated at Normal light or dark conditions at 22°C or 37°C for 1 h. Total extracted soluble protein were prepared and separated on SDS-PAGE gel and probed with anti-STY8 or anti-STY17 Ig. D) Quantification of immunoblotting was performed with ImageJ software (National Institute of Health). Data show the mean \pm s.e.m.; $n = 3$. Statistical significance was determined by Students t-test. A P value <0.05 was considered statistically significant compared to untreated control. Asterisks indicate statistical significance.

3.2. Characterization of the ACT domain of STY kinases

3.2.1. ACT domain regulates STY kinases

To investigate the role of the ACT domain in regulating kinase activity, ACT domain deletions of *STY8* (*STY8* Δ ACT), *STY17* (*STY17* Δ ACT), and *STY46* (*STY46* Δ ACT) were cloned into a pET21a⁺ vector, expressed in *E. coli*, and purified via a C-terminal His tag on Ni²⁺-Sepharose (schematically represented in Figure 9A). Kinase autophosphorylation compared with the wild-type variants was investigated by radioactive labeling. All Δ ACT deletion mutants displayed hyper autophosphorylation to a similar extent compared to their WT variants (Figure 9B). To investigate whether the enhanced autophosphorylation also affects target phosphorylation, we incubated the WT kinases and their Δ ACT mutant variants with pSSU. In addition we also used kinase mutants in which the threonine in the activation segment was replaced by an alanine, which renders loss of autophosphorylation activity, as a negative control (Lamberti, et al., 2011). Δ ACT mutants were able to phosphorylate pSSU to a higher extent than the WT kinase, which is in line with the higher autophosphorylation levels (Figure 9C).

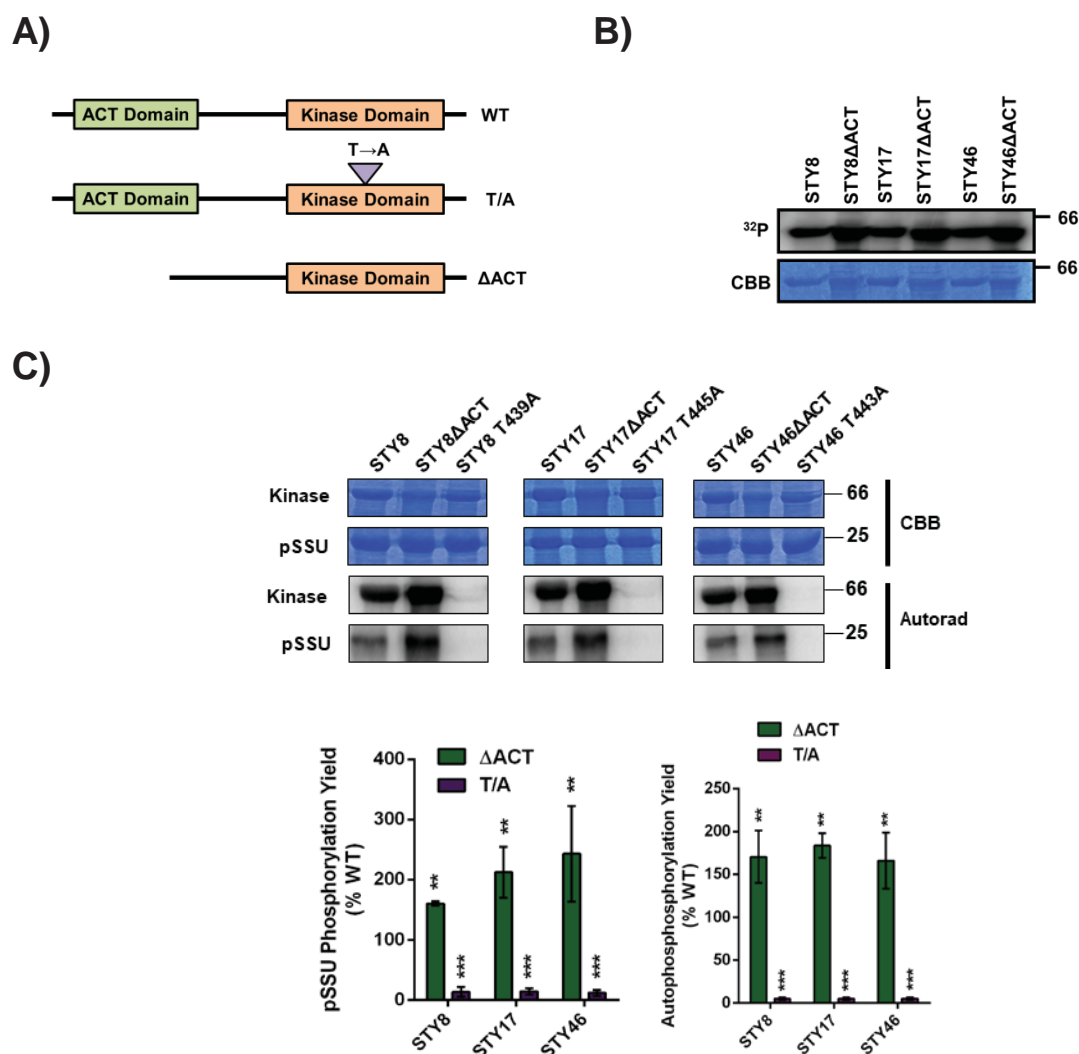


Figure 9: The ACT domain regulates STY kinase activity *in vitro*. A) Schematic representation of the constructs used in this study. Construct diagrams are not drawn to scale. B) ACT domain of STY kinases negatively regulates kinase autophosphorylation *in vitro*. Kinase assay comparing the activity of 1 μ g *E. coli* purified WT STY8, STY17, and STY46 and ACT domain deleted-variants of each kinase. A Coomassie blue gel shows equal loading of proteins. C) Conserved threonine in the activation segment (position 439 in STY8, 445 in STY17, and 443 in STY46) was substituted by an alanine in all three kinases and leads to complete loss of activity, was used as a negative control as shown in an *in vitro* kinase. Kinases and their mutant variants at 1 μ g and 2 μ g of pSSU were used for the reactions. Coomassie blue staining showing the purified proteins (top two panels) are shown and autoradiographs (bottom two panels). Hyperphosphorylation of the STY8 and phosphorylation of precursor is observed in the ACT-deleted mutant. All assays were repeated at least three times (n=3). Data show the mean \pm s.e.m.; n = 3. Statistical significance was determined by Student's t-test. A P value <0.05 was considered statistically significant compared to full-length wild-types. Asterisks indicate statistical significance.

We next sought to analyse the contribution of the ACT domain to the cytosolic distribution of the kinases. We transiently expressed all WT kinases as well as Δ ACT deletion mutants fused to green fluorescent protein (GFP) under control of the 35S promoter in tobacco leaves. The leaves were infiltrated with *Agrobacterium* containing the construct, and protoplasts were isolated 2 d after the transfection. GFP fluorescence, as well as chlorophyll autofluorescence was detected in isolated protoplasts with a confocal laser-scanning microscope (Figure 10). The GFP signal of all WT kinases was exclusively localized to the cytosol, which is consistent to literature findings (Lamberti, et al., 2011). Interestingly, when comparing the WT localization to the Δ ACT deletion mutants, they showed completely different localization patterns. The localization of the Δ ACT deletion mutant was completely changed from uniform to punctate distribution. These results suggest that the ACT domain may affect the localization of the STY kinases.

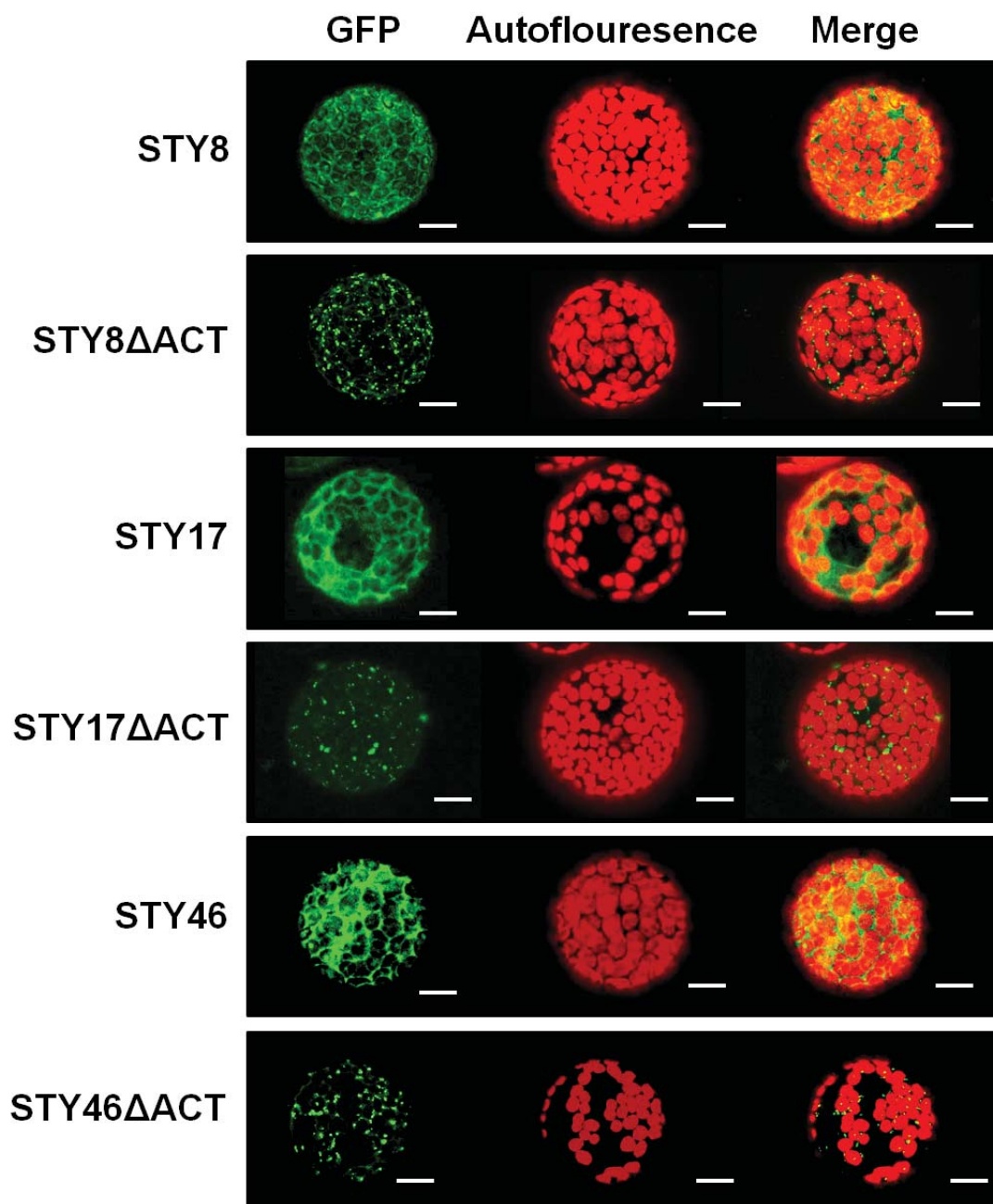


Figure 7: ACT domain determines localization distribution pattern of STY kinases.

Transient expression of WT Δ ACT deletion kinases fused with GFP in tobacco. Protoplasts were isolated after the transfection, and fluorescence was observed at 488 nm. GFP fluorescence was shown in green, and chlorophyll autofluorescence is shown in red. (Scale bar: 10 μ m.)

To evaluate binding dynamics of the kinase and its substrate, we employed MST. MST is a sophisticated method to directly monitor protein-protein interaction in solution by tracking the movement of proteins in a temperature gradient. Usually, a fluorescence tag is coupled to one of the targets and upon binding, the altered movement behavior is detected. Hence, by adding an increasing concentration of the binding partner, minor changes of the hydration shell can be audited. Subsequently, binding curves are deduced from the changes in

fluorescence response. STY8 and STY8 Δ ACT were coupled to the fluorescent tag, and increasing amounts of precursor pSSU were used as analytes. Interestingly, precursor pSSU binding to STY8 Δ ACT ($K_D=4.2 \pm 2.5$ nM) was stronger than to WT STY8 ($K_D=8.08 \pm 2.5$ nM) (Figure 8). To investigate whether the autophosphorylation state of the kinase affects binding affinity to pSSU we used STY8 T439A, a mutant that renders loss of autophosphorylation activity (Lamberti, et al., 2011). Indeed, we obtained the weakest binding affinities of STY8 T439A with pSSU ($K_D=708$ nM) (Figure 11). These data suggest an important role of phosphorylation in formation of the kinase-precursor complex.

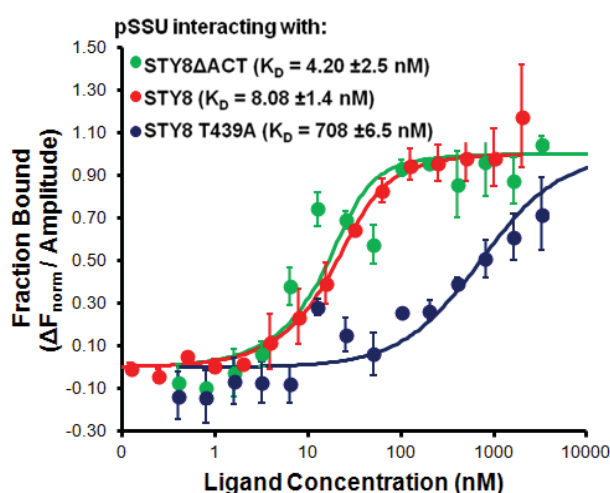
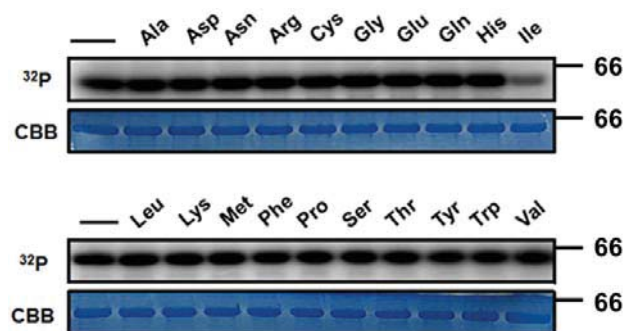


Figure 11: ACT domain plays a role in formation of the kinase-precursor complex. Thermophoretic mobility was monitored between pSSU and WT STY8 (red), and STY8 Δ ACT (green) and STY8 T439A (blue) mutants. Kinase variants (from 0.1 nM to 3 μ M) was applied to a constant fluorescence labeled pSSU (25 nM). Weakest interaction was observed between pSSU and STY8 T439A mutant when compared to WT STY8 (K_D of 708 nM and 8 nM, respectively). Strongest interaction was observed between pSSU and STY8 Δ ACT mutant ($K_D = 4$ nM). $n = 3$.

3.2.2. STY8 is negatively regulated by Ile via the ACT domain

Since many ACT domains are known to bind to amino acids, we conducted radioactive kinase assays with STY8 and 20 amino acids at a final concentration of 5 mM. Quantifying the kinase activity via its autophosphorylation levels, we identified Ile to negatively regulate kinase autophosphorylation (Figure 12). In Figure 13A we used varying amounts between 0-5 mM Ile added to a STY8 autophosphorylation assay, showing decreased autophosphorylation with increasing amounts of Ile.

A)



B)

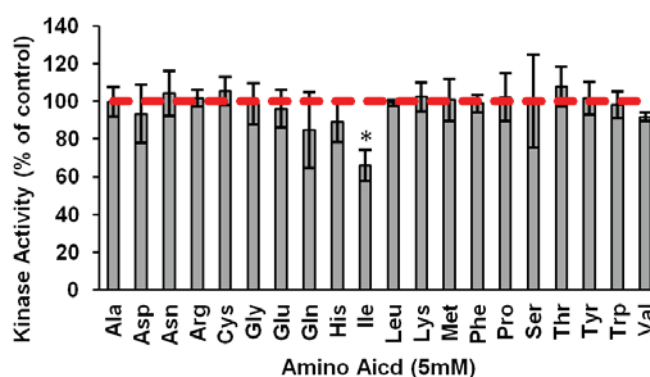
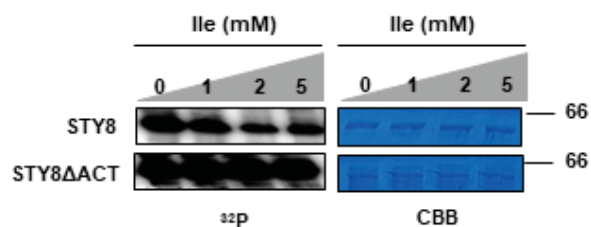


Figure 12: Ile negatively regulates STY8 autophosphorylation *in vitro*. A) Kinase assay comparing the activity of 0.25 μg *E. coli* purified STY8 in presence of 5 mM of various amino acids. Significant decrease in autophosphorylation is observed in presence of Ile. A Coomassie blue gel shows equal loading of proteins. B) Quantification of kinase assays was performed with ImageQuant software (GE Healthcare). All assays were repeated at least three times. $n = 3$. Data show the mean \pm s.e.m. Statistical significance was determined by Students t-test. A P value < 0.05 was considered statistically significant compared to untreated control. Asterisks indicate statistical significance.

In order to investigate whether the ACT domain is responsible for Ile sensitivity, we conducted a radioactive kinase assay with STY8 and STY8 Δ ACT in presence of increasing concentration of Ile. We observed loss of Ile sensitivity in the ACT deletion mutant, indicating that Ile binding occurs within the ACT domain (Figure 13A). To analyze the binding constant between the kinases and Ile we employed MST. STY8 and STY8 Δ ACT were coupled to the fluorescent tag, and increasing amounts of Ile were used as analytes. Indeed, we observed a binding event using WT STY8 ($K_D = 311 \mu\text{M}$). However, no binding curve could be fitted using STY8 Δ ACT, supporting the idea of the ACT domain has an Ile binding site (Figure 13B). To further investigate whether interaction with Ile is also dependent on the state of the autophosphorylation site, we used STY8 T439A to investigate Ile binding (Figure 13B).

Interestingly, no binding was observed, suggesting Ile binding to the ACT domain is influenced by the status of the activation segment.

A)



B)

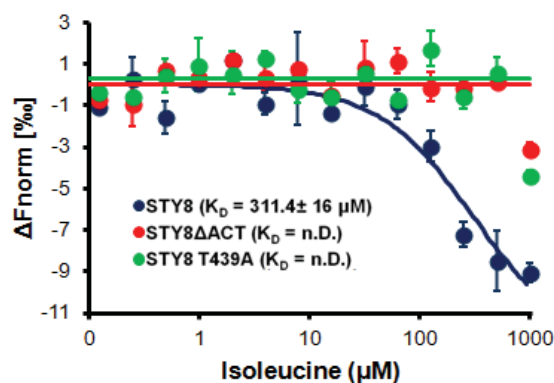


Figure 13: Ile binds to STY8 via the ACT domain. A) Kinase assay comparing the activity of *E. coli* purified STY8 WT or STY8 Δ ACT mutant in presence of increasing concentrations of Ile (1,2 and 5 mM). WT STY8 sensitivity to Ile is increased in a concentration dependent manner. A Coomassie blue gel shows equal loading of proteins. B) Thermophoretic mobility was monitored. Ile (from 30 nM to 1 mM) was applied to a constant fluorescence labeled STY8 (blue),and STY8 Δ ACT (red) and STY8 T439A (green)(25 nM). Weak interaction was observed between STY8 and Ile ($K_D = 311 \mu M$). No interaction between Ile and both mutants was observed ($K_D = n.D.$). $n = 3$.

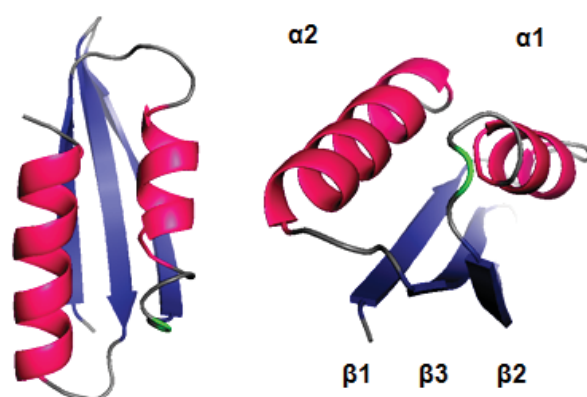
3.2.3. ACT domain Protein alignment of STY8, STY17 and STY46 and selected proteins

Typically, ACT domains display a $\beta\alpha\beta\beta\alpha\beta$ secondary structure motif (Chipman & Shaanan, 2001; Grant, 2006). Structural determination of ACT domain proteins revealed a conserved amino acid binding interface between the alpha helices and beta sheets within the ACT domain (Grant, 2006). Furthermore, multiple sequence alignments of several ACT domain proteins revealed a conserved glycine that might play an important role in amino acid binding coordination (Figure 14A). This glycine has been shown to be primarily located between the first beta sheet and the first alpha helix. Furthermore, glycine to aspartate mutation analysis of the ACT domain containing Aspartate Kinase revealed a significant loss of amino acid sensitivity (Y. Kikuchi et al., 1999). In order to identify such a conserved glycine in the STY kinases, we aligned the ACT domain protein sequences of all three STY kinases. Using PSSpred server (University of Michigan) to predict protein secondary structure and AlignX/ClustalW for protein sequence alignment revealed that the ACT domains of the STY kinases lacked a fourth beta-sheet after the second alpha helices structure. We have identified a conserved glycine at amino acid positions at positions 197 for STY8, 203 for STY17, and 201 for STY46. In contrast to the other selected proteins, this particular glycine is located between the first alpha helices and the second beta sheet and, hence, could be potentially responsible for Ile affinity (Figure 14A). In addition, we used Pymol visualization tools to visualize the location of the conserved glycine (Figure 14B). The particular glycine (coloured in green, Figure 14B) is located at a loop that may form a binding interface for Ile affinity.

A)

Protein/sp	residues	beta 1	alpha 1	beta 2	beta 3	alpha 2	beta 4	
AspKi_Ath	340-419	NVTMDIASTRMLGQVGF	LAKVFSIFEELG	-ISVDVVATSEVSISL	LDPSKLWSRELIQQEL	DHVVEELEKIAV	NLIKG----79	
PheOH_rat	35-110	ISLFSLKEE-----V	GALAKVLR	LNFENDILNTH-IESR	PSRLNKDEYEFFTYL	DKRTKPV	LGSIKSKRNDIGATVHEL	SRDKEK--79
ThrD_Ec	338-407	EALLAVTIPE---EK	GSFLKFCQLLCCR----	SVTEFN	YRFADAKNACIFV	GVRLSRGL	EERKEILQMLNDGGYS	VVDLS----73
PGDH_Ec	338-409	--RLMHIHEN--RP	GVLTALNK	IFAEQGVNIAAQV	LQTSAQMGYVVIDI	AEDVAEKALQ	AMKAIPG----	TIRARLLY----72
STY8_Ath	172-239	--MHEITFSTIDKPK	LLSQLTSL	LGELGLNIQ	EAHAFSTVDGFSLD	VFVVDGWSQE	ETDGLRDALSKEIL-----	68
STY17_Ath	178-244	MHEITFSTIDRPK	LLSQLTSM	LGELGLNIQ	EAHAFSTADGFSLD	VFVVDGWSQE	ETGLKDALKKEIR-----	68
STY46_Ath	176-241	--LHEITFSTEDKPK	LLFQLTALL	AELGLNIQ	EAHAFSTTDGYSLD	VFVVDGW	PYEETERLRISLEKEAA-----	68

B)



C)

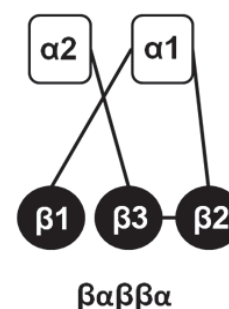
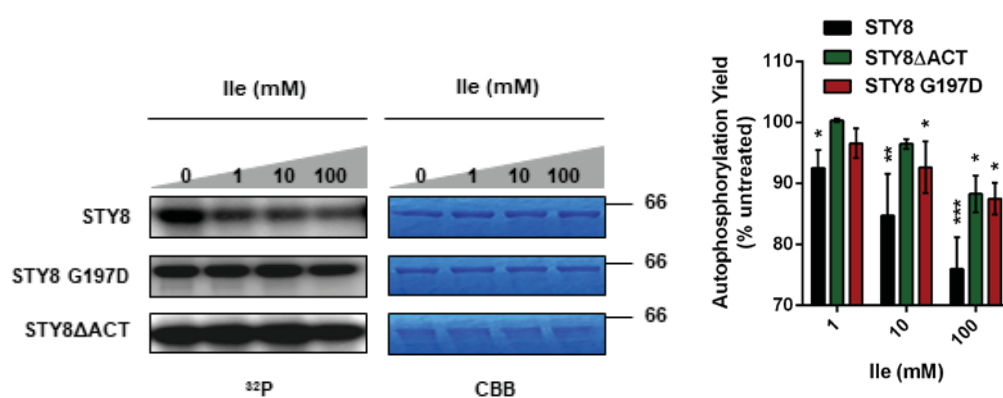


Figure 14: ACT domain protein alignment of STY8, STY17 and STY46 and selected proteins. A) The sequences of the ACT domains were aligned with regard to residue type and secondary structure. Within the ACT domain, the conserved glycine residues responsible for amino acid sensitivity are colored in black for the STY kinases (position 197 in STY8, 203 in STY17 and 201 in STY46) and selected proteins. The protein abbreviations are: PGDH, D-3-phosphoglycerate dehydrogenase; PheOH, phenylalanine hydroxylase; AspKi, aspartate kinase; ThrD, threonine deaminase. The species abbreviations are: Ec, *E. coli*; rat, *Rattus norvegicus*; Ath, *Arabidopsis thaliana*. B) The three-dimensional structure prediction of the ACT domain of STY8. The domain structure was visualized using PyMOL molecular visualization tool. The α -helices, β -sheets, loop regions, and the predicted conserved glycine are shown in pink, yellow, blue, grey, and green colors, respectively. C) Schematic representation of the secondary structure motif of the ACT domain of the STY kinases.

In order to study the importance of this glycine, we substituted it by aspartate and performed radioactive kinase assay and compared its Ile sensitivity to WT STY8 and STY8 Δ ACT mutant (Figure 15A). Interestingly, we observe Ile insensitivity in the STY8 G197D mutant, similar to STY8 Δ ACT. However, in high concentrations of Ile, we observed loss of Ile

insensitivity (Figure 15A). To confirm these bindings dynamics between the kinases and Ile we employed MST. STY8, STY8 Δ ACT, and STY8 G197D were coupled to the fluorescent tag, and increasing amounts of Ile were used as analytes (Figure 15B). Indeed, we observed a binding event using WT STY8 ($K_D = 311 \mu\text{M}$). Weaker binding affinities were observed between STY8 G197D and Ile ($K_D = 999 \mu\text{M}$). No binding curve could be fitted using STY8 Δ ACT. Overall, the results suggests that this particular region is responsible for Ile specificity

A)



B)

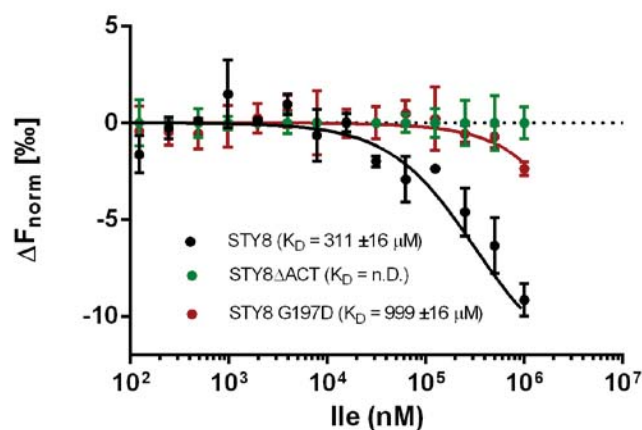
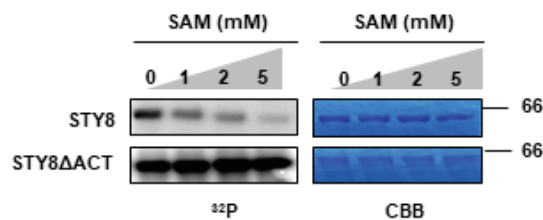


Figure 15: A conserved glycine is involved in Ile binding . A). Kinase assay comparing the activity of *E. coli* purified STY8 WT, and STY8 Δ ACT and STY8G197D mutants in presence of increasing concentrations of Ile. The specific activity of the purified kinase in absence of Ile is defined as 100%. WT STY8 show concentration dependent sensitivity to Ile (blue). Glycine to Aspartate mutation variant (red) show comparable insensitivity to the ACT-deleted mutant (green). B) Quantification of kinase activities. All assays were repeated at least three times. $n = 3$. Data show the mean \pm s.e.m.; Statistical significance was determined by Students t-test. A P value <0.05 was considered statistically significant compared to untreated control. Asterisks indicate statistical significance. C) Thermophoretic mobility was monitored upon Ile (from 30 nM to 1mM) was applied to a constant fluorescence labeled STY8 (blue) and STY8 Δ ACT (green) and STY8 G197D (red)(25 nM). Weak interaction was observed between STY8 and Ile ($K_D = 311 \mu\text{M}$). Weaker interaction between STY8 G197D ($K_D = 999 \mu\text{M}$). No interaction between Ile and STY8 Δ ACT was observed ($K_D = \text{n.D.}$). $n = 3$.

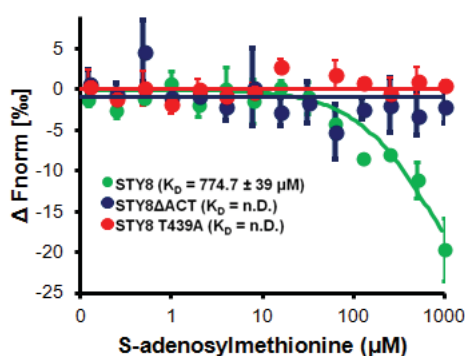
3.2.4. STY8 is negatively regulated by S-Adenosylmethionine via the ACT domain

It has been previously been reported that, along with amino acids, ACT domains also interact with various metabolites derived from amino acids. Using radioactive kinase assays, we incubated various metabolites with *E. coli* purified STY8 (data not shown). Here, we identified S-adenosylmethionine (SAM) to significantly down regulate STY8 autophosphorylation (data not shown). To examine whether SAM down regulates kinase activity via the ACT domain, we incubated increasing amounts of SAM with STY8 and STY8 Δ ACT and compared autophosphorylation activity (Figure 16A). The activity of STY8 Δ ACT showed SAM-resistance, implying that SAM negatively regulates STY8 via its ACT domain. To investigate the binding event in more detail we conducted MST analysis with SAM and STY8, STY8 Δ ACT or STY8 T439A. A weak binding affinity could be calculated for STY8 ($K_D = 775 \mu\text{M}$), whereas no binding of SAM to STY8 Δ ACT was observed (Figure 16B). To further investigate whether interaction with SAM also is dependent on the state of the autophosphorylation site, we used STY8 T439A to investigate Ile binding (Figure 13B). Interestingly, no binding was observed, suggesting SAM binding to the ACT domain is influenced by the status of the activation segment. To verify further that the metabolite binding is conferred by the ACT domain, we used the recombinant ACT domain to perform MST analysis with Ile and SAM. Interestingly, the K_D values were enhanced to $81.48 + 34 \mu\text{M}$ for Ile and to $47.28 + 25 \text{ nM}$ for SAM (Figure 3F). This result confirms that both metabolites are bound by the ACT domain. The differences observed in binding affinities using the full length proteins versus the isolated ACT domain might indicate that steric hindrances occur in measurements with the full-length proteins thus leading to lower accessibility for the metabolites. To confirm specificity of the binding event, we included methionine as a negative control. No binding event could be observed for these measurements (Figure 3F).

A)



B)



C)

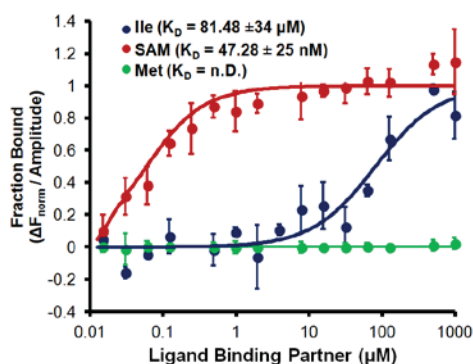


Figure 16: SAM binds to STY8 via the ACT domain. A) Kinase assay comparing the activity of *E. coli* purified STY8 WT or STY8 Δ ACT mutant in presence of increasing concentrations of SAM (1,2 and 5 mM). WT STY8 sensitivity to Ile is increased in a concentration dependent manner. Coomassie blue gel shows equal loading of proteins. B) Thermophoretic mobility was monitored upon SAM (from 30 nM to 1mM) was applied to a constant fluorescence labeled STY8 (green) and STY8 Δ ACT (blue) and STY8 T439A (red)(25 nM) (Upper graph). Weak interaction was observed between STY8 and Ile ($K_D = 311 \mu\text{M}$). No interaction between SAM and both mutants was observed ($K_D = \text{n.D.}$). C) Thermophoretic mobility was monitored upon SAM (red), Ile (blue), or Met (green) (from 30 nM to 1 mM) was applied to a constant fluorescence labeled ACT domain of STY8. Weakest interaction was observed between ACT domain and Ile when compared to SAM (K_D of 81 μM 47 nM and, respectively). No interaction with Met was detected. $n = 3$.

3.2.5. Conserved Glycine in the ACT domain of STY8 does not play a role in S-Adenosylmethionine sensitivity

To verify whether the STY8 G197D mutant is also insensitive to SAM, a kinase assay was performed in presence of increasing concentration of SAM with STY8 Δ ACT also being used as a negative control (Figure 17). In contrast to Ile, we observed SAM sensitivity in both WT and the STY8 G197D mutant. To confirm these bindings dynamics we between the kinases and SAM we employed MST. STY8, STY8 Δ ACT, and STY8 G197D were coupled to the fluorescent tag, and increasing amounts of Ile were used as analytes (Figure 15B). Indeed, we observed a binding event using WT STY8 ($K_D = 774 \mu\text{M}$). Similar binding affinities was observed between STY8 G197D and SAM ($K_D = 785 \mu\text{M}$). By and large, our data indicated that the conserved glycine located in the loop region between the first alpha helix and the second beta sheet is only responsible for Ile binding.

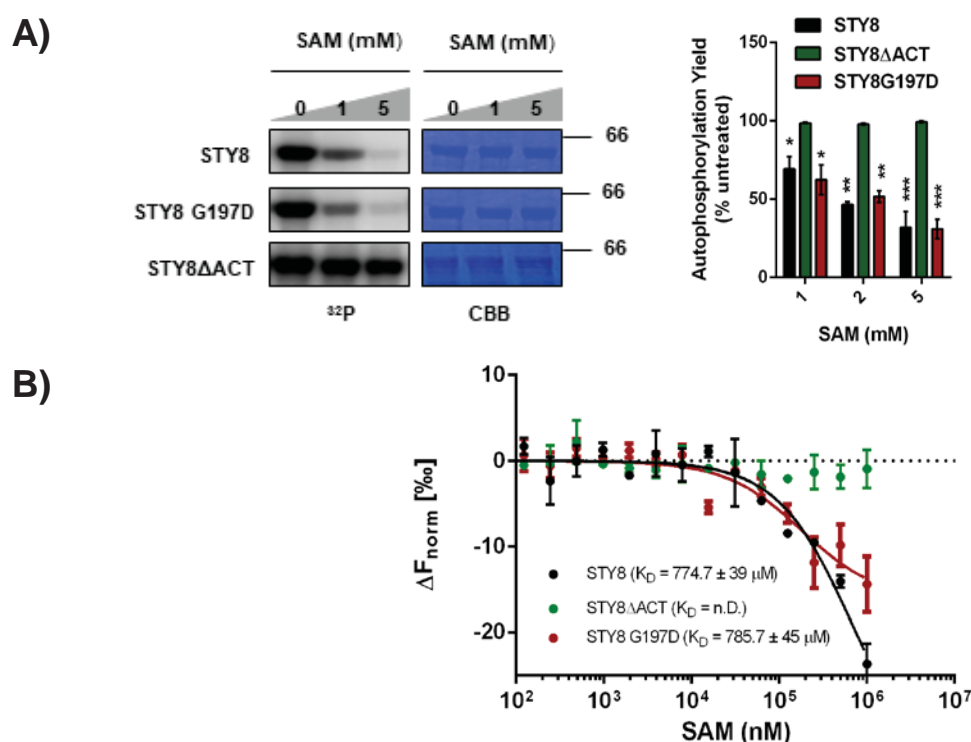
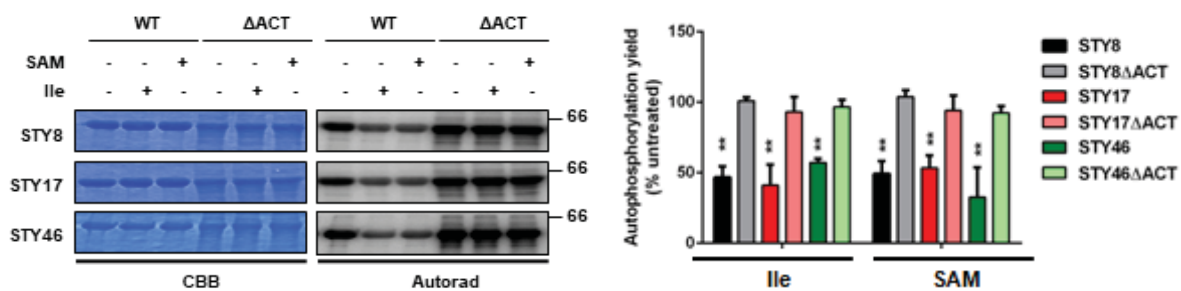


Figure 17: Conserved Glycine in the ACT domain does not play a role in SAM sensitivity. Kinase assay comparing the activity of *E. coli* purified STY8 WT, and STY8 Δ ACT and STY8G197D mutants in presence of increasing concentrations of S-Adenosylmethionine. A Coomassie blue gel shows equal loading of proteins. WT STY8 and STY8 G197D show equal concentration dependent sensitivity to S-adenosylmethionine. Quantification of all blots performed using ImageJ. Data show the mean \pm s.e.m.; $n = 3$. Statistical significance was determined by Students t-test. A P value < 0.05 was considered statistically significant compared to untreated control. Asterisks indicate statistical significance. B) Thermophoretic mobility was monitored upon SAM (from 30 nM to 1 mM) was applied to a constant fluorescence labeled STY8 (blue), and STY8 Δ ACT (green) and STY8 G197D (red)(25 nM). Weak interaction was observed between STY8 and SAM ($K_D = 774 \mu\text{M}$). Similar interaction between STY8 G197D ($K_D = 785 \mu\text{M}$). No interaction between Ile and STY8 Δ ACT mutants was observed ($K_D = \text{n.D.}$). $n = 3$.

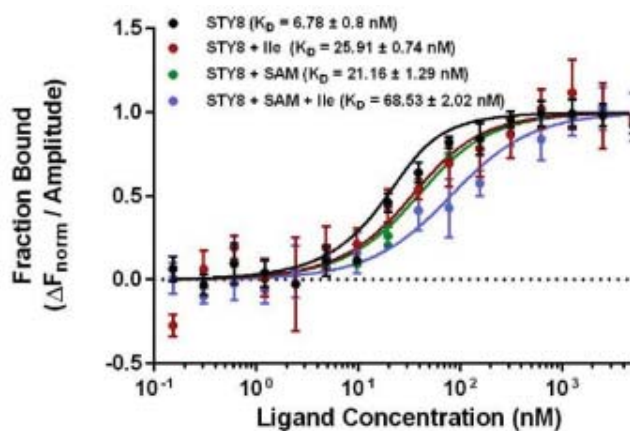
3.1.1. SAM and Ile inhibit precursor affinity and phosphorylation by STY8

To confirm whether all STY kinases show equal sensitivity to either SAM or Ile, we conducted a kinase assay using the WT and Δ ACT mutant kinase in presence of either SAM or Ile. Our data indicates equal sensitivity to SAM and Ile across all WT kinase tested. No autophosphorylation changes was observed in all Δ ACT mutant variants. To investigate the effect of the increases kinase autophosphorylation by SAM and Ile on pSSU binding, we performed MST (Figure 18B). Strong binding of pSSU to STY8 was observed ($K_D=6.7$ nM). A three-fold increase in dissociation constant was observed in presence of Ile ($K_D = 21.2$ nM). Approximately four-fold increase was detected in presence of constant amount of SAM ($K_D = 25.7$ nM). Weakest binding affinity was observed in constant combined presence of SAM and Ile ($K_D=68.5$ nM). To investigate the binding inhibition effects of SAM and Ile on the precursor pSSU phosphorylation by STY8 we conducted an in vitro kinase assay (Figure 18C). Here, observe similar precursor phosphorylation inhibition when precursor was incubated with SAM and Ile independently. In addition, minor negative effects on the STY8 autophosphorylation is also observed. However, when precursor pSSU, SAM, and Ile were incubated simultaneously, complete abolishment of kinase autophosphorylation and precursor phosphorylation was observed. These results suggest that STY8 autophosphorylation and precursor phosphorylation seems to be synergistically regulated by both SAM and Ile via the ACT domain.

A)



B)



C)

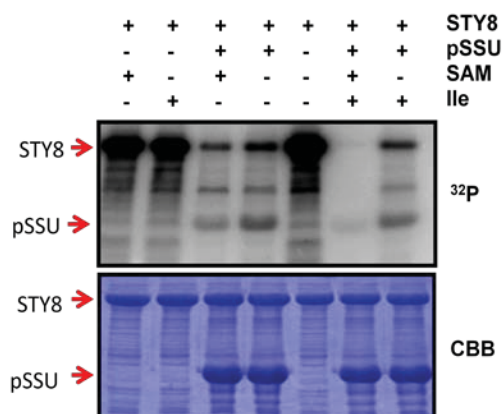
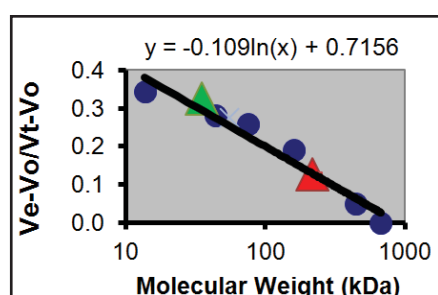
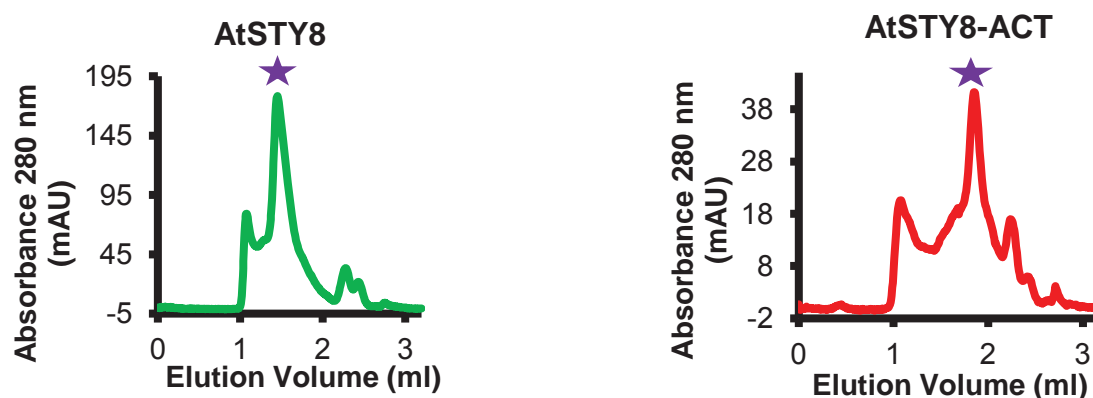


Figure 18: SAM and Ile synergistically inhibit precursor phosphorylation by STY8. A) Kinase assay comparing the activity of *E. coli* purified WT STY kinases, and Δ ACT mutant variant in presence of either 5 mM of S-adenosylmethionine or 5 mM Ile. All WT Kinases show equal sensitivity to either S-adenosylmethionine and Ile. A Coomassie blue gel shows equal loading of proteins. All blots were repeated at least three times. Quantification of all blots performed using ImageJ. Data show the mean \pm s.e.m.; $n = 3$. Statistical significance was determined by Students t-test. A P value <0.05 was considered statistically significant compared to untreated control. Asterisks indicate statistical significance. B) Thermophoretic mobility was monitored upon STY8 in presence of SAM and/or Ile (1 mM) was applied to a constant fluorescence labeled pSSU (25 nM). Weakest interaction was observed between pSSU and STY8 in presence of both SAM and Ile (light blue, K_D of 68.5 nM) when compared to independent incubations of SAM and isoleucine (red, K_D of 25.9 nM and dark blue 21.2 nM, respectively). Strongest interaction was observed between pSSU and STY8 alone ($K_D = 6.7$ nM). $n = 3$. C) Kinase assay comparing the activity of *E. coli* purified STY8 WT in presence of pSSU, SAM, and/or Ile. Phosphorylation level of pSSU by STY8 was lowest in presence of both SAM and isoleucine (panel 6). All assays were repeated at least three times.

3.1.2. STY8 and the ACT domain form oligomers

Several ACT domain containing proteins have been isolated as large multimeric protein complexes with ACT domains associating into dimers, trimers or even tetramers (Reviewed by Grant 2006). To elucidate the oligomeric state of the recombinant STY8 protein we employed size-exclusion chromatography (SEC). Our results showed that STY8 eluted at 217 kDa, which suggests formation of a trimer or tetramer (Figure 19). To investigate the role of the ACT domain in the oligomerization state of STY8, we analyzed only the ACT domain, which was purified as recombinant protein of 35 kDa. Our results indicated that the purified ACT domain of STY8 likewise elutes as a trimer or tetramer, due to the apparent size of 35 kDa (Figure 19). Overall, our SEC analysis strongly indicates that the ACT domain is essential for kinase oligomerization. To further analyze the oligomerization state of the purified STY8, the purified enzyme was examined in both denaturing (SDS-PAGE) and non-denaturing (Native PAGE) conditions. In denaturing conditions, purified STY8 displayed an apparent molecular weight of approximately 60 kDa, consistent with the theoretical value calculated based on the amino acid sequence (red arrow). Native-PAGE showed that STY8 exhibited significantly at a molecular weight of about 210 kDa, which corresponds to our findings from our SEC measurements. This strongly suggests that the active protein oligomerizes to either a trimer or a tetramer confirmation.

A)



Color Code	Protein	Size (kDa)	Oligomer state
Green	ACT domain	35	Trimer/tetramer
Red	STY8	217	Trimer/tetramer

B)

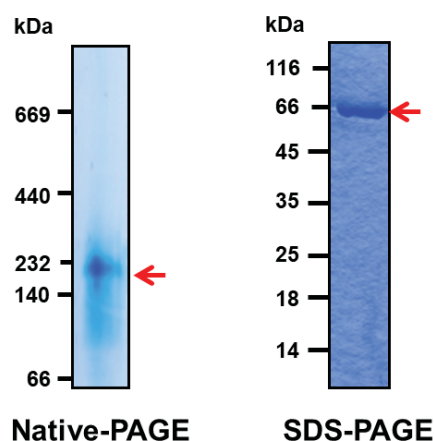
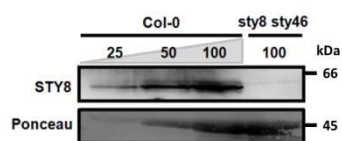


Figure 19: Oligomerization analysis of AtSTY8 and AtSTY8-ACT Proteins were over-expressed and purified from *E. coli* and analyzed using size exclusion chromatography using a Superdex 200 increase 3.2/300 column. The purple star represents elution volume. The Kav ($V_e - V_o / N_t - V_o$) versus LogMW plot with the equation of the line for superdex standards is shown Calibration plot with the corresponding sizes for different standard proteins used are shown in dark blue circles (described in the methods). Stars represents various variants of STY8 used in this study: Green AtSTY8-ACT, Red AtSTY8. Table of summary is displayed. $n=3$. B) SDS and Native-PAGE analysis of the purified STY8 (marked in red). All blots repeated at least three times.

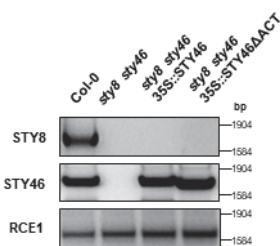
3.1.3. Generation and characterization of *sty8 sty46/35S::STY46ΔACT* deleted *Arabidopsis* mutant

To study the role of the ACT domain *in planta*, we used the *sty8 sty46* double mutant and complemented the line with *STY46ΔACT* under control of the 35S CMV promoter (*35S::STY46ΔACT*) (Figure 20). The gene expression levels in the generated lines were confirmed using reverse transcription (RT)-PCR and quantitative real-time PCR (Figure 20B and 20C). Growth phenotypes of WT, *sty8 sty46*, *35S::STY46* and *35S::STY46ΔACT* were analyzed under fluorescent long day light (16 h of light), white light-emitting diode (LED) normal light ($125 \mu\text{mol photons m}^{-2} \text{s}^{-1}$) and fluctuating light (240 s of low light (LL, $55 \mu\text{mol}\cdot\text{m}^{-2}\cdot\text{s}^{-1}$) and 120 s of high light (HL, $700 \mu\text{mol}\cdot\text{m}^{-2}\cdot\text{s}^{-1}$) alternately cycled, for 3 weeks after germination. For soil based phenotype analysis, we investigated the bolting time and leaf area. In terms of bolting time, the double mutant showed significant delay in bolting time when compared to the WT (Figure 20G). *35S::STY46* rescued the bolting time phenotype. Interestingly, the deletion of the ACT domain did in fact slightly reduce the bolting time when compared to the full length complementation. For leaf area studies, we measured the leaves of all lines 3 weeks after stratification. We observed significant reduction in leaf area in the double mutant when compared to the WT (Figure 20E). Surprisingly, no major difference in leaf size was observed when comparing the full length complementation to the ΔACT deleted mutant.

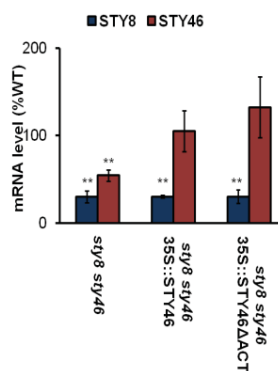
A)



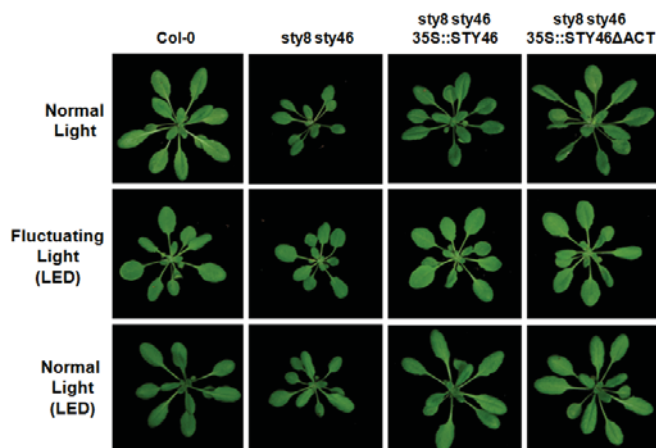
B)



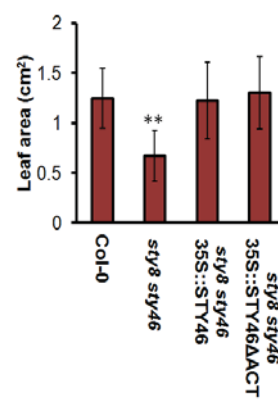
C)



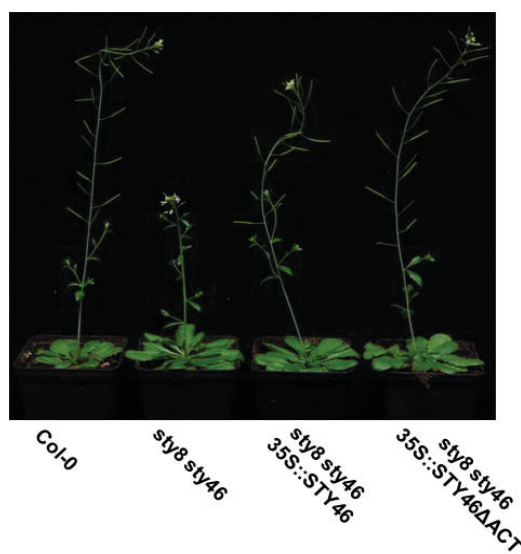
D)



E)



F)



G)

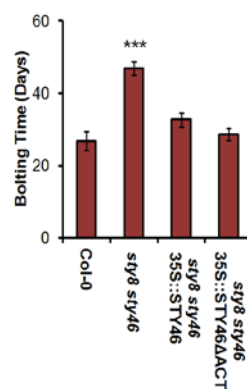
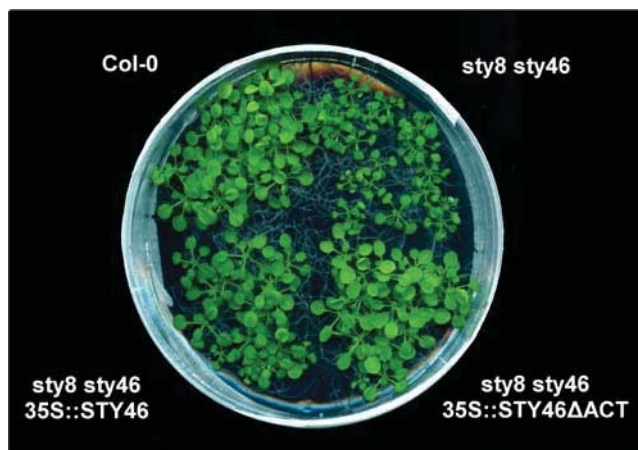


Figure 20: Generation of STY46 Δ ACT complemented lines and of the *sty8 sty46* mutants: A) Immunoblot analysis of STY8 in *sty8 sty46*. For 100%, 20 μ g of protein was loaded on a 12% SDS gel, transferred to a polyvinylidene difluoride membrane, and immunodecorated with specific STY8 antisera. Ponceau staining of the large subunit of Rubisco is shown as a control. B) RT-PCR analysis of the WT, *sty8 sty46*, and *sty8 sty46/35S-STY46*, and *sty8 sty46/35S-STY46 Δ ACT* demonstrating the expression of STY8 and STY46 in all lines. C) STY46 Δ ACT lines in the background of *sty8 sty46* were analyzed by quantitative RT-PCR with STY8 and STY46 specific oligonucleotideoligonucleotides. Values were calculated relative to housekeeping gene RCE1 and expression levels relative to the WT are given. D) Phenotype analysis of wild-type, mutant and complemented lines grown on different light regimes. Plants are shown 4 weeks after germination on soil. E) Total leaf area of 21 days old plants. Area of leaf of wild-type (Col-0) plants and, *sty8 sty46/STY46* complementation, and *sty8 sty46/STY46 Δ ACT* mutant plants, n=15 leaves from each line. All Quantification of leaves were performed using ImageJ. Data show the mean \pm s.e.m.; Statistical significance was determined by Students t-test. A P value <0.05 was considered statistically significant compared to the WT. Asterisks indicate statistical significance. F) Flowering phenotype of wild-type and mutant plants 5 weeks after germination. Flowering time of plants grown are presented in number of days to bolting. Bolting time of wild-type (Col-0) plants, *sty8 sty46/STY46* complementation, and *sty8 sty46/STY46 Δ ACT* mutant. n=15 plants from each line. Data show the mean \pm s.e.m. Statistical significance was determined by Students t-test. A P value <0.05 was considered statistically significant compared to the WT. Asterisks indicate statistical significance

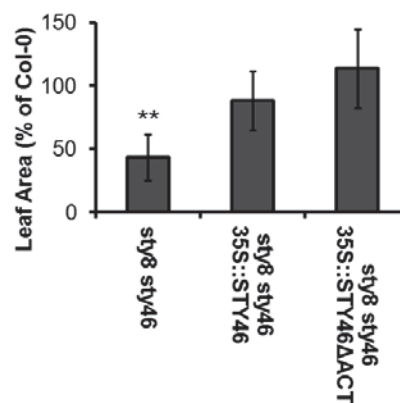
3.1.4. Deletion of the ACT domain does not effects leaf size and root length on plates.

To confirm the findings observed with soil-grown plants, we germinated all lines on MS plates with sucrose for 21 days and 10 days and quantified the leaf area and root length, respectively (Figure 21). In terms of leaf area, the double mutant shows significant reduction in leaf area. Full length complementation shows full recovery of the phenotype. Deletion of the ACT domain shows does not affect leaf area values when compared to full length complementation (Figure 21A). In terms of root length, the double mutant showed significantly reduced root growth when compared to the WT (Figure 21C). Again, the full length complementation rescued the phenotype. The ACT deletion mutant complementation shows no significant differences in root length when compared to the full length complementation. Overall, no significant phenotype is observed when all lines were germinated on plates. The phenotype on plates were comparable to the soil based studies.

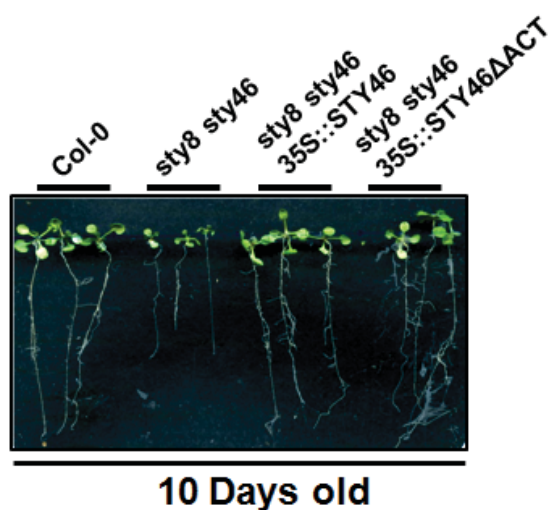
A)



B)



C)



D)

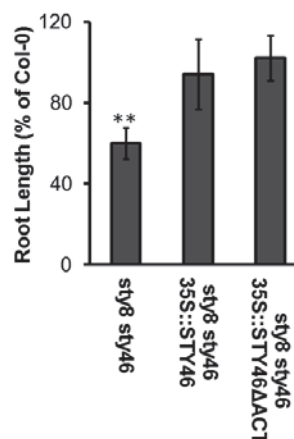


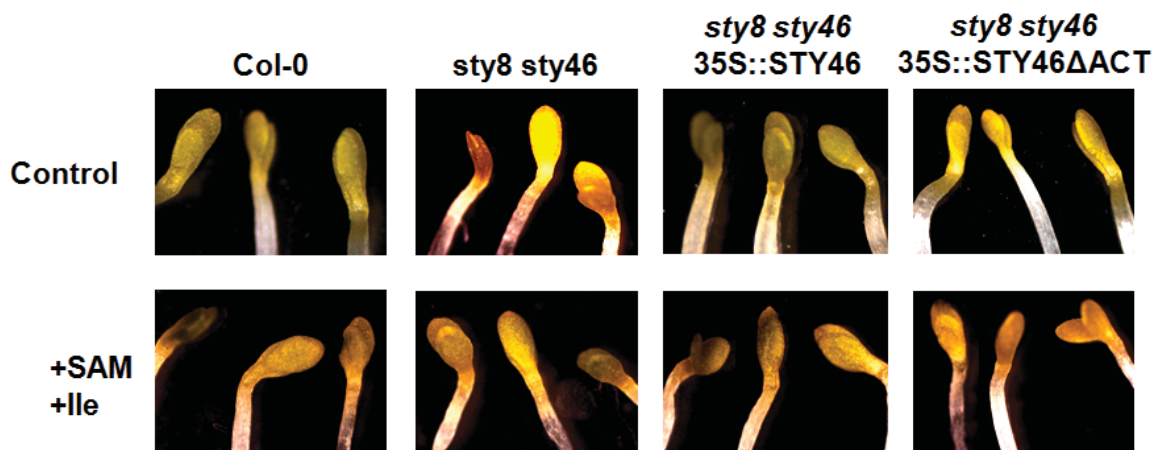
Figure 21: Plate Based phenotype analysis of mutant plants. A) Phenotypes on MS plates. B) All Quantification of leaves were performed using ImageJ. Data show the mean \pm s.e.m. Statistical significance was determined by Students t-test. A P value <0.05 was considered statistically significant compared to the WT. Asterisks indicate statistical significance. C) Three representative seedlings of the WT (Col-0), *sty8 sty46*, *sty8 sty46/35S::STY46*, and *sty8 sty46/35S::STY46ΔACT* mutants roots of 10-d-old seedlings grown vertically on MS plates. D) Root length quantification relative to WT. $n=15$. Data show the mean \pm s.e.m. Statistical significance was determined by Students t-test. A P value <0.05 was considered statistically significant compared to the WT. Asterisks indicate statistical significance

3.1.5. Deletion of the ACT domain affects chlorophyll accumulation during greening

In order for proper differentiation from etioplast to chloroplast to take place, manifold of preproteins are required for thylakoid formation. To study chlorophyll accumulation, Col-0, *sty8 sty46*, *sty8 sty46/35S::STY46*, and *sty8 sty46/35S::STY46 Δ ACT* mutants were grown in darkness for 6 d and subsequently transferred to light for several hours to investigate possible differences during chloroplast differentiation (Figure 22). The greening process was delayed in the *sty8 sty46*, which corresponds to previous studies (Lamberti, et al., 2011). We observed no changes between the full complementation and the WT. Interestingly, the greening process was also delayed in *sty8 sty46/35S::STY46 Δ ACT* mutant comparable to *sty8 sty46* mutant as observed by coloring of the cotyledons as well as by quantitative measurements of the chlorophyll *a* and *b* contents 4 h after the transition to light.

To investigate the role of SAM and Ile in the greening process, Col-0, *sty8 sty46*, *sty8 sty46/35S::STY46*, and *sty8 sty46/35S::STY46 Δ ACT* mutants were grown in darkness on MS plates with 8 μ M SAM and 100 μ M Ile for 6 d and subsequently transferred to light for 4 hours to investigate possible differences during chloroplast differentiation (Meng et al., 2018; Schertl et al., 2017). Interestingly, the WT showed reduced chlorophyll accumulation. Interestingly, the double mutant showed also reduction in chlorophyll accumulation. The full length complementation showed similar SAM/Ile sensitivity trends when compared to the WT. However, the ACT deletion complementation showed no significant change when compared to the untreated. Our data indicates that the ACT domain is essential for metabolite and amino acid sensitivity in plants.

A)



B)

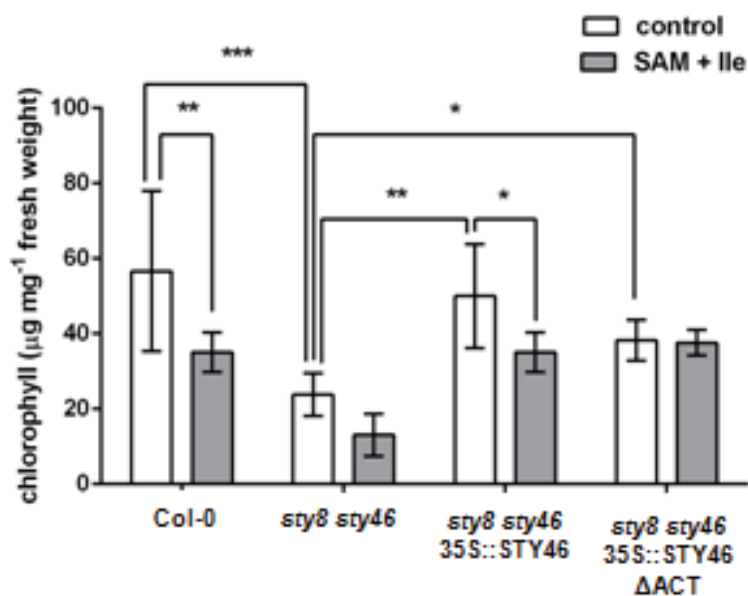


Figure 22: Greening is delayed in Δ ACT kinase mutant plants. A) Three representative seedlings of the WT (Col-0), *sty8 sty46*, *sty8 sty46/35S:STY46*, and *sty8 sty46/35S:STY46 Δ ACT* are shown 4 h after illumination when grown on MS plates supplemented with 8 μ M SAM and 100 μ M Ile. B, Chlorophyll concentration was measured 4 h after exposure of etiolated seedlings to light (100 μ E m⁻² s⁻¹). Chlorophyll concentration was measured in μ g mg⁻¹ fresh weight. Significant decrease in chlorophyll content in *sty8 sty46* was observed. Full and partial was observed in *sty8 sty46/35S:STY46* and *sty8 sty46/35S:STY46 Δ ACT*, respectively. However, in plates supplemented with SAM and Ile, significant reduction in chlorophyll content was observed in all lines except for *sty46/35S:STY46 Δ ACT*. (n=3). All assays were repeated at least three times. Data show the mean \pm s.e.m. Statistical significance was determined by Student's t-test. A P value <0.05 was considered statistically significant compared to the WT. Asterisks indicate statistical significance

3.1.1. Deletion of the ACT domain effects phosphorylation status of precursors in planta.

To investigate whether hyper-phosphorylation of the kinase and its substrates could also be observed with *sty8 sty46/35S::STY46ΔACT* plant extracts, we performed kinase assays using soluble protein extracts of WT plants, *sty8 sty46* double mutants, *sty8 sty46/35S::STY46* and *sty8 sty46/35S::STY46ΔACT* complementation plants to study the phosphorylation potential of recombinant pSSU. Precursor phosphorylation was reduced in the *sty8 sty46* double mutant compared to WT, as expected (Figure 23). Residual phosphorylation in *sty8 sty46* is most likely due to the redundant function of STY17. However, the precursor phosphorylation yield was higher in *sty8 sty46/35S::STY46ΔACT* in comparison to WT as well as to *35S::STY46*. We therefore conclude that the STY46ΔACT functions *in planta* in a comparable manner to the recombinant purified protein.

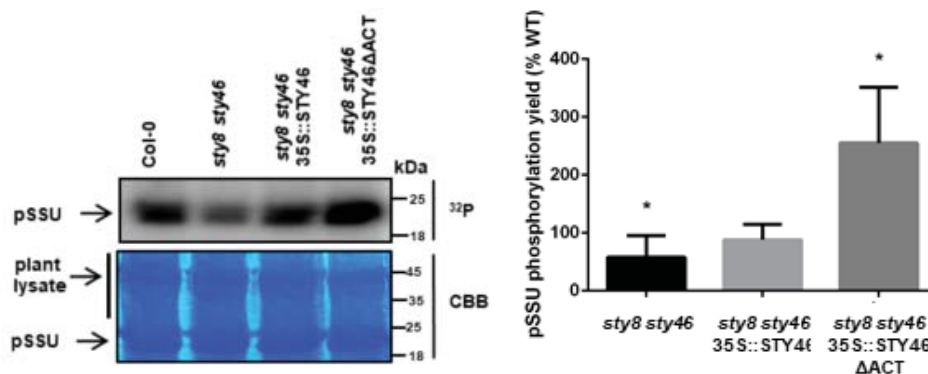


Figure 23: Precursor phosphorylation yield is increased in Δ ACT kinase mutant plants. Soluble protein extract isolated from WT (*Col-0*), *sty8 sty46*, *sty8 sty46/35S::STY46* and *sty8 sty46/35S::STY46ΔACT* was used to phosphorylate pSSU. A coomassie stained gel is shown to depict equal loading (CBB). All assays were repeated at least three times ($n=3$). Quantification of blots performed in ImageJ. Data show the mean \pm s.e.m. Statistical significance was determined by Student's t-test. A P value <0.05 was considered statistically significant compared to the WT. Asterisks indicate statistical significance

4. Discussion

4.1. Role of Acclimation in protein import into chloroplast

As a consequence of several environmental factors, plants have evolved to sense and acclimate to a variety of different biotic and abiotic stress conditions. Hence, the understanding of the molecular switches has been of particular interest for field-grown plants. Recently, it has been shown that the protein content of the chloroplast alters in response to short term exposure to changing temperature or light conditions (Dutta et al., 2009; Grimaud et al., 2013). This strongly indicates that the plant acclimation response is triggered by external stimuli. Furthermore, changes in protein organeller composition alters the supply of photosynthetic complexes needed to ensure optimal performance. Since the majority of chloroplast proteins is encoded in the nucleus and translated as preproteins in the cytosol, posttranslational targeting is a first crucial step towards providing these organelles with the required proteins. This process requires strict regulation of the posttranslational modifications, such as phosphorylation of preproteins in the cytosol. The cytosolic kinases STY8, STY17 and STY46 have been isolated from *Arabidopsis thaliana* as kinases responsible for transit peptide phosphorylation (Lamberti, et al., 2011; Martin, et al., 2006)

4.1.1. High Temperature decreases precursor phosphorylation yield

We investigated the effects of temperature on the phosphorylation of precursors *in vitro*. Interestingly, chill conditions alone did not affect precursor phosphorylation yield. Furthermore, the ATP-driven import of precursor of pSSU into plastids was shown to be down-regulated by 49% in chill-stressed plants (Dutta et al., 2009). Interestingly, we observed a significant decrease in precursor phosphorylation when plants were exposed to higher temperature. This also goes in line in with previous studies showing a significant reduction in protein import in plants exposed to higher temperatures (Dutta et al., 2009). We also detected a significant decrease in kinase expression in short term high temperature conditions. This coincides the decrease in precursor phosphorylation yield. Both of these finding suggest that the guidance complex formation efficiency is reduced in unstable temperature conditions due to the lack of precursor phosphorylation activity preformed by the kinases. Possibly, as a consequence, impaired chlorophyll biosynthesis and chloroplast development was observed (Kumar Tewari & Charan Tripathy, 1998). This leads to reduced photosynthesis and, hence, a significant loss of plant productivity.

4.1.2. Light increases precursor phosphorylation and STY kinase expression

Upon observing negative effects of precursor phosphorylation and kinase expression in temperature acclimating conditions, we investigated the effects of varying light conditions. We observed a significant increase in precursor phosphorylation and kinase expression in high light acclimating conditions. In addition, when combined high light and chill conditions, we still observe increase in precursor phosphorylation. This indicates that light is the predominant factor in changes in precursor phosphorylation. The double mutant kinase deletion showed significant reduction in precursor phosphorylation in normal light and high light conditions. This reaffirms the role of the kinases in precursor phosphorylation. Furthermore, studies have shown that the import efficiency of some precursors are affected by different light conditions (Hirohashi et al., 2001). Here, they show two Ferredoxin isoproteins: pFdI and pFdIII, to have two distinct light-dependent import regulation patterns. pFdI, a photosynthetic ferredoxin precursor, was efficiently imported into the stroma in both the light and in the dark. In contrast, pFdIII, a non-photosynthetic ferredoxin precursor, was mostly mis-targeted to the intermembrane space of chloroplastic envelopes as an unprocessed precursor form in the light but was efficiently imported into the stroma and processed to its mature form in the dark. In addition to the role of light as a possible regulatory signal, it also suggests that photosynthetic activity (and thereby the reduced environment via the decreased $\text{NADP}^+/\text{NADPH}$ ratio) can affect the import efficiency (reviewed by Kovacs-Bogdan, et al., 2010).

4.1.3. STY kinases phosphorylated precursors that associate with HSP70 and/or 14-3-3.

Chloroplast preprotein import into chloroplast is an energy-demanding process. Once synthesized, some preproteins require additional stabilizing cofactors/molecules to ensure efficient and correct targeting. Hence, most chloroplast precursor proteins contain characteristics to bind the heat shock chaperone protein HSP70 (May & Soll, 2000). In addition to HSP70, it has also been shown that small 14-3-3 acidic proteins can bind a subset of chloroplast preproteins (Fellerer, et al., 2011).. Formation of the guidance complex have been shown to prevent aggregation and enhance the import rate of the preproteins (May & Soll, 2000). Furthermore, phosphorylated preproteins have been shown to display higher affinity to 14-3-3. Out of a randomly selected population of preproteins, approximately 25% were found to associate with 14-3-3 (Fellerer, et al., 2011). In addition, it has been postulated that precursors shown to exclusively interact with HSP70 might later on form complexes with 14-3-3 or HSP90. Our *in vitro* studies in which we incubated STY8 with selected precursors that have been shown to exclusively interact with 14-3-3 and/or HSP70

indicated that some precursors may have more than a single targeting mechanism. All selected 14-3-3 associated precursors have been shown to be phosphorylated by STY8. Precursors such as pFNRL1, pHCF101, pCAB1, pClp2, and pLHCb2 that have been shown to exclusively interact with HSP70, are also phosphorylated by STY8. This implies that precursor import into chloroplast is a dynamic process and various import mechanism may be utilized during different developmental phases or as a response to various environmental factors. Since the kinases involved in the phosphorylation of the precursor also need to be regulated to maintain proper influx of precursors during chloroplast biogenesis, we pursued to characterize features that make these kinases distinct from its other family members.

4.2. The role of the ACT domain in STY Kinase activity

The unique feature that distinguishes these kinases from other protein kinases, is that it harbors a special domain upstream of its highly conserved kinase domain. Using a BLAST search of this unique domain, a high sequence homology with the ACT domain has been observed. This domain was initially identified in three enzymes: aspartate kinase-chorismate mutase-TyrA (prephenate dehydrogenase) (Aravind & Koonin, 1999; Chipman & Shaanan, 2001; Curien et al., 2008). Since its identification, the ACT domains was shown to be present in several amino acid biosynthetic enzymes.

4.2.1. *In vitro* characterization of the ACT domain of STY kinase

4.2.1.1. The ACT domain regulates spatial distribution and kinase activity

To investigate the role of ACT domain in kinase localization, we expressed a GFP-tagged proteins and its deletion mutants and analyzed protein localization by confocal microscopy. Although both mutant and wild-type maintain the cytosolic localization, we observed significant alteration in localization pattern. The distribution pattern changed from uniform to punctuate distribution. Furthermore, we also show that the substitution of a threonine in the activation segment of the kinase domain to an alanine, which renders the kinase inactive, does not alter spatial distribution pattern when compared to its active form (data not shown). This suggests that the ACT domain influences the protein cellular localization and thereby might alter the phosphorylation of its substrates.

To study the role of the ACT domain on kinase activity, the ACT domain was deleted and kinase activity was tracked *in vitro*. The deletion of the ACT domain in all kinases lead to a significant increase of kinase autophosphorylation. When incubated in presence of the precursor pSSU, significant increase in precursor phosphorylation yield was also observed. Using microscale thermophoresis, we observed a slight change in the binding affinity between the kinase and precursor when the ACT domain was deleted. In addition, the kinase

in its inactive form resulted in a decrease in kinase affinity to substrate. This indicated the importance of autophosphorylation for the conformational change required for kinase-substrate interaction and any modification might destabilize the active conformation leading to the loss of kinase activity (Nolen et al., 2004). This also suggests that the kinase undergo an in cis autophosphorylation process (Lamberti, et al., 2011; Lochhead, 2009).

4.2.1.2. Ile and SAM regulates kinase activity via the ACT domain

Several small molecules, including amino acids and purines, have been shown to interact and negatively regulate enzyme activity via the ACT domains in other species. All ligands have been shown to bind at different regions of the ACT domain, and hence have one or more regulatory effects. Serine has been shown to negatively regulate 3-phosphoglycerate dehydrogenase, which is an enzyme required at the committed step in the phosphorylated pathway of L-serine biosynthesis in *E. coli* (Schuller et al., 1995; Thompson, et al., 2005). Tyrosine has also been shown to negatively regulate Prephenate dehydrogenase, an essential enzyme in the pathway to synthesize tyrosine in *B. subtilis* and *Aquifex aeolicus* (Nester & Jensen, 1966; Sun et al., 2009). Formyl FH₄ hydrolase, 10-formyltetrahydrofolate (formyl-FH₄) to FH₄ and formate in *E.coli*, is negatively regulated by glycine, and it is also up regulated by methionine (Nagy et al., 1995). Threonine deaminase, a key enzyme in the branched-chain amino acid synthesis, is down regulated by Ile and up regulated by valine *S. typhim* (Gallagher et al., 1998). Phenylalanine hydroxylase, which is involved in phenylalanine catabolism (and, to some extent, tyrosine biosynthesis) in rats, is negatively regulated by tetrahydrobiopterin and up regulated by phenylalanine (Mitnaul & Shiman, 1995). Finally, the *A.thaliana* Acetohydroxyacid synthase, which catalyzes the initial step in the formation of the branched-chain amino acids, is negatively regulated by both Ile and valine at two different sites of its ACT domain (Lee & Duggleby, 2002). In our studies, we identified SAM and isoleucine to negatively regulate STY kinase activity and consequently precursor phosphorylation via the ACT domain. The precursor of SAM, methionine, is synthesized from aspartate in the chloroplast. SAM synthesis is an energy demanding process in which the entire triphosphate chain is displaced from ATP by SAM synthetase and pyro- and orthophosphate, respectively (Singh et al., 1995). SAM is used as a methyl group carrier required to modify DNA and RNA. It has also been suggested that the ACT domains could also bind nucleotides (Mas-Droux et al., 2006). Interestingly, no binding of either SAM or Ile was observed in the inactivated STY kinase. Furthermore, we also show that a conserved glycine between the first alpha helices and second beta sheet is essential for Ile binding but not SAM. Hence, the interaction of SAM and Ile with the ACT domain may be required for the inhibition under specific physiological conditions. Our data suggests Ile and SAM binding to the ACT domain is influenced by the status of the activation segment and that it inhibits the kinase domain in a synergistic manner. Binding of either molecule could

cause disruption of the precursor substrate binding site of the kinase domain. An active kinase may liberate the ACT domain, exposing particular regions for binding. SAM, alongside with lysine, has also been shown to inhibit Aspartate kinase in *Arabidopsis* (Mas-Droux, et al., 2006). It has been shown that a loop in the ACT domain may be involved in the binding of Lys and SAM provides an explanation for the synergistic inhibition by these effectors. Our data suggest that the confirmation of the ACT domain of STY kinase may operate in a similar fashion in presence of its interacting partners.

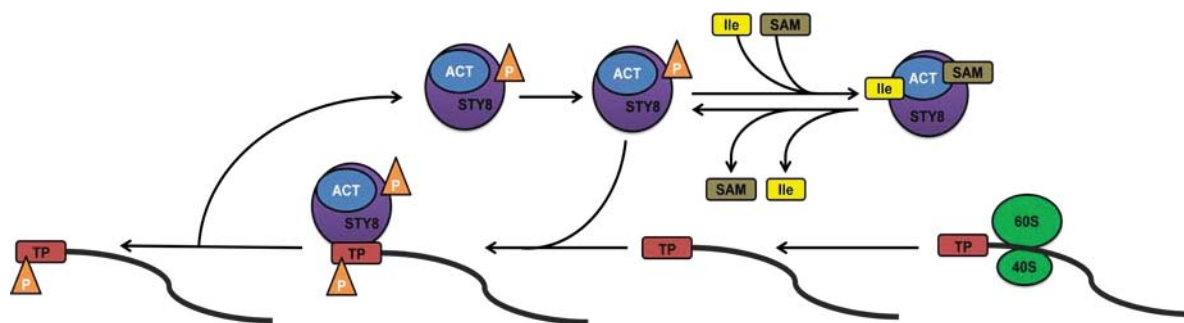


Figure 23: Model of the regulation of the STY kinase. Preproteins are translated in the cytosol with a cleavable transit peptide (TP). Once synthesized, active STY kinases bind and phosphorylate the preproteins at specific serine/threonine residues at the transit peptide. Active kinase liberates from phosphorylated precursor before import. Kinases phosphorylation of precursor is inhibited by presence of cytosolic Ile (Ile) and SAM (SAM). Ile and SAM binding to specific regions of the ACT domain initiates a new folding confirmation rendering inactivation of the activation segment within the kinase domain.

4.2.1.3. ACT domain of STY8 involved in oligomerization

ACT domains have been identified in many proteins with varying number of repeats and oligomerization states. So far, at least 10 ACT domain-containing proteins structures have been determined, and five of these have been solved with bound ligand (reviewed by Grant, 2006; Lang, et al., 2014). Despite few numbers of structures characterized, they display diverse modes in which the domains associate with each other. Proteins containing one or more ACT domains have been isolated and displayed 2, 3, or 4 oligomeric features across different species. To name a few: *E. coli* d-3-phosphoglycerate dehydrogenase was isolated as a tetramer (Schuller, et al., 1995; Thompson, et al., 2005). The *A. thaliana* aspartate kinase as a dimer (Mas-Droux, et al., 2006), the *M. tuberculosis* ATP phosphoribosyltransferase as a hexamer (Cho, et al., 2003; Lohkamp, et al., 2004), *E. coli* threonine deaminase is isolated as a tetramer (Gallagher, et al., 1998), thiamine binding protein from *B. subtilis* YkoF was isolated as dimer (Devedjiev, et al., 2004), and rat phenylalanine hydroxylase also as dimer (Kobe et al., 1999). Our data indicated that STY8 forms a trimer or a tetramer. The stand-alone ACT domain of STY8 was also isolated a trimer or a tetramer. This suggests that the active form of kinases may need to undergo

oligomerization to become active. The ability of the STY kinases to oligomerize adds another degree of complexity to their regulation and substrate specificity. Dimerization of non receptor kinases is not particularly novel as it is also observed in many up-stream acting kinases (reviewed in Pelech, 2006). Some of these kinases have tandem catalytic domains (such as SgK069 - a human encoded NFK1 kinase, GCN2 - general control nonderepressible 2, MSK1 and MSK2 - Mitogen- and stress-activated protein kinase-1/2, and RSK1-4 - p90 ribosomal S6 kinase family), whereas at least 59 others have been reported to dimerize or oligomerize. Furthermore, homology studies predicted at least another 36 protein kinases are likely to also undergo complex formation either through homo- and heterodimeric catalytic kinase domain interactions (Pelech, 2006).

4.2.2. *In vivo* characterization of the ACT domain of STY kinase

4.2.2.1. The ACT domain influences etioplasts to chloroplast transition in cotyledons

Polygenetic analysis of STY8, STY17, and STY46 homologs in plants show that there are indeed homologs found in all green land plants (i.e. green algae, mosses, ferns, monocots, and dicots), except for species containing rhodoplasts or complex plastids (Lamberti, et al., 2011). Furthermore, the analysis showed that STY8 and STY17 are very closely related and are located in a larger context of duplicated genes, as verified with the Plant Genome Duplication Database (Lamberti, et al., 2011; Tang et al., 2008). In depth studies show that STY kinases 8, 17, and 46 play an important role chloroplast biogenesis during greening (Lamberti, et al., 2011). To investigate the role of the ACT domain of the STY kinases in the greening process, the *sty8 sty46* double mutant was complemented with the full length coding sequence of STY46 (*35S::STY46*) and the ACT deleted variant (*35S::STY46 Δ ACT*) expressed under the 35S promoter. When grown under standard light conditions, the *35S::STY46* complementation rescued the double mutant phenotype. However, *35S::STY46 Δ ACT* did not show a no obvious phenotype when compared to the *35S::STY46* complementation. However, when the greening process was analyzed, it was observed that the transition from etioplast to chloroplast was indeed affected in both the double mutant and the *35S::STY46 Δ ACT* complementation. The *35S::STY46* complementation rescued the greening process. After 4 h of light exposure, chlorophyll content was reduced by 40% in both the double mutant and the ACT domain deletion. *35S::STY46* complementation showed complete recovery in chlorophyll content. Previous data have shown that expression of the essential PSII assembly factor HCF136 with a phosphomimicking variant only partially rescued the seedling lethal *hcf136* phenotype (Nickel et al., 2015). This suggests that

enhanced transit peptide phosphorylation does reduce import of precursors which significant effect in cotyledons, whereas mature leaved developed similar to WT (Lamberti, et al., 2011)

4.2.2.2. Linking SAM and Ile to Chloroplast function

In plants, when methionine is synthesized in the chloroplast and exported to the cytosol, it is converted to SAM. No data to date could demonstrate an alternative location of SAM synthesis in plants. SAM has been shown to play a role in several major processes in plants (Ravanel et al., 2004; Ravanel et al., 1998; Sauter et al., 2013). Primarily, the bulk of methionine is converted into SAM by a transmethylation reaction. SAM is used as a precursor of lignin, choline and its derivatives, and pectin (methyl esters of polygalacturonic acid) for plant structural components. In addition, the carbon backbone is used as a precursor to the plant hormone ethylene, polyamines, and in the chain elongation pathway of glucosinolate biosynthesis. Ile is also predominantly synthesized in the chloroplast from threonine. Data showing a link between SAM and Ile is limited in plants. However, there has been evidence shown that using *Corynebacterium glutamicum* strains that over-produce Ile, yielded increases of SAM production. This suggests a possible co-production mechanism in place regulating SAM and Ile (Han et al., 2015). In addition, threonine synthesis from *A. thaliana* and other plants is allosterically activated by SAM (Curien et al., 1998; Laber et al., 1999; Madison & Thompson, 1988). Through promoting threonine synthesis, extracellular SAM may indirectly upregulate Ile production. In order for this to occur, SAM needs to be recycled to regenerate methionine. Through a proposed carrier-mediated process, SAM is transported into chloroplasts by facilitated diffusion (Ravanel, et al., 2004; Ravanel, et al., 1998). Once SAM is transported in the chloroplast, it is converted to S-adenosylhomocysteine (SAH) in the stroma by specific methyltransferase activities. SAH is either used to regenerate methionine or it is removed from the chloroplast using the same uniport carrier in a given condition. These processes are required to maintain methylation reactions and other SAM-dependent functions in the chloroplasts, and therefore, essential for chloroplastic one-carbon metabolism (reviewed by (Hanson & Roje, 2001).

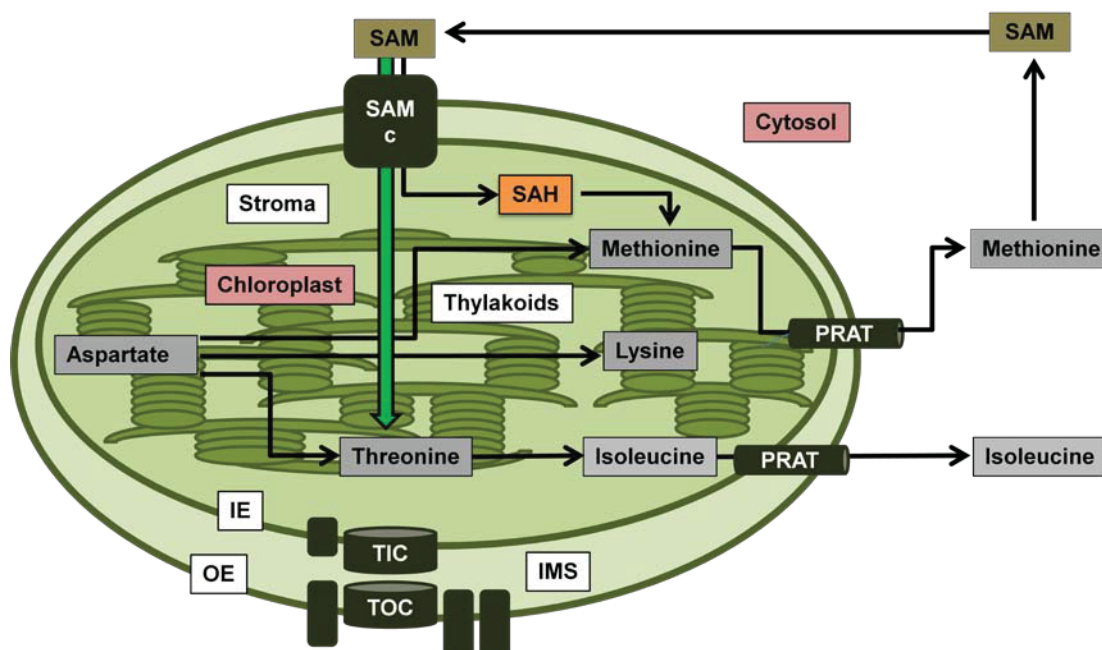


Figure 24: Proposed regulatory mechanism of aspartate amino acid synthesis: All aspartate-derived amino acids (grey) are synthesized in the chloroplast in plastids. SAM-cycle reactions take place in both the cytosol and chloroplast. Once methionine is exported from the chloroplast via specific Protein Amino Acid Transporter (PRAT), it is converted to SAM (SAM) by SAM Synthase. SAM may also be imported into the stroma of the chloroplast in a facilitated diffusion process via a carrier (SAMc). Once in the stroma, SAM is converted to S-adenosylhomocysteine (SAH) by a specific methyltransferase. In a multi-step process SAH is converted to methionine by SAH hydrolase and methionine Synthase. In specific conditions, SAM may stimulate the synthesis of threonine. Threonine also gives rise to Ile. Ile can be exported from the chloroplast via PRATs.

4.2.2.3. The role of SAM and Ile inhibits kinase activity during etioplasts to chloroplast transition in cotyledons

When the greening process of WT, double mutant, *35S::STY46* and *35S::STY46 Δ ACT* complementation was analyzed in presence of SAM and Ile, significant reduction of chlorophyll content was observed across all lines except for the *35S::STY46 Δ ACT* complementation. In fact, no change in chlorophyll content was observed in the Δ ACT complementation when compared to the full length complementation. This may suggest that the intracellular concentration of these small molecules can directly impact the STY kinase activity, hence providing an additional layer of stringent control on the current model of protein import into chloroplast. In a given condition when excess concentration of SAM is produced, it causes an inhibition of key enzymes in the synthesis of aspartate derived-amino acids (reviewed by Joshi & Jander, 2009). We therefore propose that the observed negative effect caused by SAM and Ile treatment is indeed due to kinase inhibition. The *sty8 sty46* also showed a reduction in chlorophyll accumulation, probably due to STY17 inhibition. Our

data indicates that metabolic regulation of the ACT domain in the STY kinases influences chloroplast biogenesis.

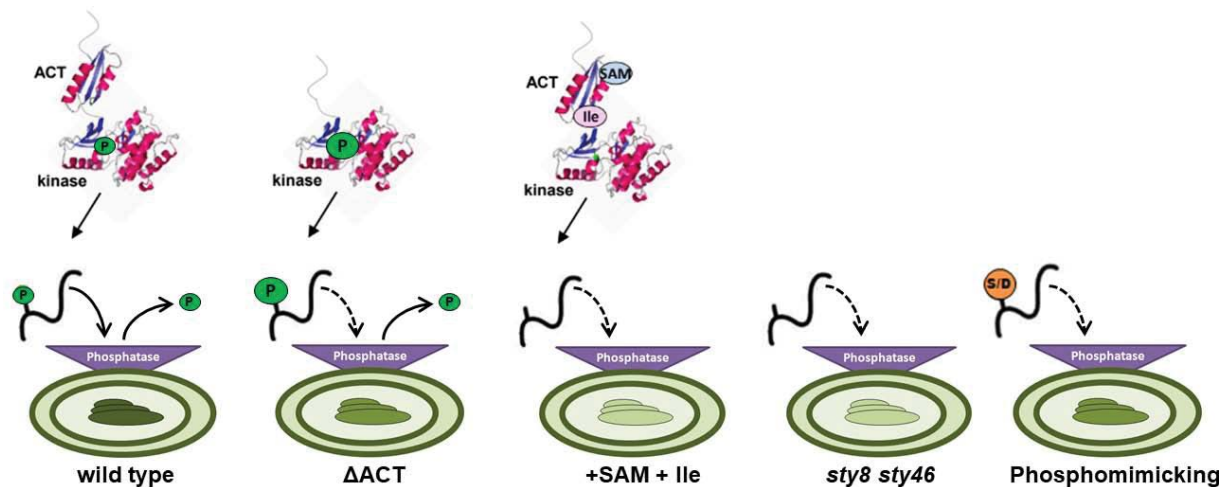


Figure 25: Schematic representation of the role of phosphorylation and regulation of STY kinase activity by the ACT domain in protein import. Predicted structures of the STY8 ACT domain as well as kinase domain are present. Autophosphorylation is represented by a green 'P'. Phosphomimicking precursor is represented by orange 'S/D'. Different intensities of green refer to etioplast to chloroplast transition efficiency. See text for details.

5. Outlook

Protein phosphorylation is part of major cascades of posttranslational modifications in eukaryotic cells and affects significant portions of all cellular processes. The chloroplast has a central role integrated into the cellular signaling and phosphorylation network in plants. Recently, a large-scale chloroplast phosphoproteome analyses in *Arabidopsis* has provided extensive insight regarding phosphorylation targets. These findings have been expanded in a list of chloroplast metabolic and regulatory functions that are potentially controlled by protein phosphorylation (Baginsky & Gruissem, 2009). In addition, further perspective into phosphorylation motifs, protein kinase activities, and substrate utilization has also been gained. Phosphorylation sites and regulation of protein kinases suggests a comprehensive and integrated signaling network modulated by the chloroplast. Defects in cotyledons and retardation in growth in the mutants, suggests any hindrance during the development of cotyledons has significant impact in general plant development. This trend has been observed in deletion mutants of several other proteins involved in chloroplast biogenesis (Albrecht et al., 2006). Furthermore, various environmental factors may affect chloroplast development due to the change in regulation of various post-translational processes required for chloroplast development. Despite significant advancement in characterizing the regulation of protein kinases *in vitro*, further investigation in their regulation in response to different biotic and abiotic factors is essential.

6. References

- Albrecht, V., Ingenfeld, A. and Apel, K. (2006). Characterization of the snowy cotyledon 1 mutant of *Arabidopsis thaliana*: the impact of chloroplast elongation factor G on chloroplast development and plant vitality. *Plant Mol Biol*, 60(4), 507-518.
- Andres, C., Agne, B. and Kessler, F. (2010). The TOC complex: preprotein gateway to the chloroplast. *Biochim Biophys Acta*, 1803(6), 715-723.
- Aravind, L. and Koonin, E. V. (1999). Gleaning non-trivial structural, functional and evolutionary information about proteins by iterative database searches. *J Mol Biol*, 287(5), 1023-1040.
- Arnon, D. I. (1949). Copper Enzymes in Isolated Chloroplasts. Polyphenoloxidase in *Beta Vulgaris*. *Plant Physiol*, 24(1), 1-15.
- Baginsky, S. and Gruissem, W. (2009). The chloroplast kinase network: new insights from large-scale phosphoproteome profiling. *Mol Plant*, 2(6), 1141-1153.
- Balsera, M., Soll, J. and Bolter, B. (2009). Protein import machineries in endosymbiotic organelles. *Cell Mol Life Sci*, 66(11-12), 1903-1923.
- Bolter, B., Soll, J., Schulz, A., Hinnah, S. and Wagner, R. (1998). Origin of a chloroplast protein importer. *Proc Natl Acad Sci U S A*, 95(26), 15831-15836.
- Bolter, B., Soll, J. and Schwenkert, S. (2015). Redox meets protein trafficking. *Biochim Biophys Acta*, 1847(9), 949-956.
- Bridges, D. and Moorhead, G. B. (2005). 14-3-3 proteins: a number of functions for a numbered protein. *Sci STKE*, 2005(296), re10.
- Bruce, B. D. (2000). Chloroplast transit peptides: structure, function and evolution. *Trends Cell Biol*, 10(10), 440-447.
- Chen, K., Chen, X. and Schnell, D. J. (2000). Initial binding of preproteins involving the Toc159 receptor can be bypassed during protein import into chloroplasts. *Plant Physiol*, 122(3), 813-822.
- Chipman, D. M. and Shaanan, B. (2001). The ACT domain family. *Curr Opin Struct Biol*, 11(6), 694-700.
- Cho, Y., Sharma, V. and Sacchettini, J. C. (2003). Crystal structure of ATP phosphoribosyltransferase from *Mycobacterium tuberculosis*. *J Biol Chem*, 278(10), 8333-8339.
- Clough, S. and Bent, A. (1998). Floral dip: a simplified method for *Agrobacterium*-mediated transformation of *Arabidopsis thaliana*. *Plant J*, 16, 745-743.
- Curien, G., Biou, V., Mas-Droux, C., Robert-Genthon, M., Ferrer, J. L. and Dumas, R. (2008). Amino acid biosynthesis: new architectures in allosteric enzymes. *Plant Physiol Biochem*, 46(3), 325-339.
- Curien, G., Job, D., Douce, R. and Dumas, R. (1998). Allosteric activation of *Arabidopsis* threonine synthase by S-adenosylmethionine. *Biochemistry*, 37(38), 13212-13221.
- de la Fuente van Bentem, S. and Hirt, H. (2009). Protein tyrosine phosphorylation in plants: More abundant than expected? *Trends Plant Sci*, 14(2), 71-76.
- Devedjiev, Y., Surendranath, Y., Derewenda, U., Gabrys, A., Cooper, D. R., Zhang, R. G., Lezondra, L., Joachimiak, A. and Derewenda, Z. S. (2004). The structure and ligand binding properties of the *B. subtilis* YkoF gene product, a member of a novel family of thiamin/HMP-binding proteins. *J Mol Biol*, 343(2), 395-406.
- Dougherty, M. K. and Morrison, D. K. (2004). Unlocking the code of 14-3-3. *J Cell Sci*, 117(Pt 10), 1875-1884.
- Dutta, S., Mohanty, S. and Tripathy, B. C. (2009). Role of temperature stress on chloroplast biogenesis and protein import in pea. *Plant Physiol*, 150(2), 1050-1061.
- Fellerer, C., Schweiger, R., Schongruber, K., Soll, J. and Schwenkert, S. (2011). Cytosolic HSP90 cochaperones HOP and FKBP interact with freshly synthesized chloroplast preproteins of *Arabidopsis*. *Mol Plant*, 4(6), 1133-1145.
- Gallagher, D. T., Gilliland, G. L., Xiao, G., Zondlo, J., Fisher, K. E., Chinchilla, D. and Eisenstein, E. (1998). Structure and control of pyridoxal phosphate dependent allosteric threonine deaminase. *Structure*, 6(4), 465-475.
- Gould, S. B., Waller, R. F. and McFadden, G. I. (2008). Plastid evolution. *Annu Rev Plant Biol*, 59, 491-517.

- Grant, G. A. (2006). The ACT domain: a small molecule binding domain and its role as a common regulatory element. *J Biol Chem*, 281(45), 33825-33829.
- Grimaud, F.,Renaut, J.,Dumont, E.,Sergeant, K.,Lucau-Danila, A.,Blervacq, A. S.,Sellier, H.,Bahrman, N.,Lejeune-Henaut, I.,Delbreil, B. and Goulas, E. (2013). Exploring chloroplastic changes related to chilling and freezing tolerance during cold acclimation of pea (*Pisum sativum* L.). *J Proteomics*, 80, 145-159.
- Han, G.,Hu, X. and Wang, X. (2015). Co-production of S-adenosyl-L-methionine and L-isoleucine in *Corynebacterium glutamicum*. *Enzyme Microb Technol*, 78, 27-33.
- Hanks, S. K.,Quinn, A. M. and Hunter, T. (1988). The protein kinase family: conserved features and deduced phylogeny of the catalytic domains. *Science*, 241(4861), 42-52.
- Hanson, A. D. and Roje, S. (2001). One-Carbon Metabolism in Higher Plants. *Annu Rev Plant Physiol Plant Mol Biol*, 52, 119-137.
- Hauenstein, M.,Christ, B.,Das, A.,Aubry, S. and Hortensteiner, S. (2016). A Role for TIC55 as a Hydroxylase of Phyllobilins, the Products of Chlorophyll Breakdown during Plant Senescence. *Plant Cell*, 28(10), 2510-2527.
- Hinnah, S. C.,Hill, K.,Wagner, R.,Schlicher, T. and Soll, J. (1997). Reconstitution of a chloroplast protein import channel. *EMBO J*, 16(24), 7351-7360.
- Hirohashi, T.,Hase, T. and Nakai, M. (2001). Maize non-photosynthetic ferredoxin precursor is mis-sorted to the intermembrane space of chloroplasts in the presence of light. *Plant Physiol*, 125(4), 2154-2163.
- Hough, R.,Pratt, G. and Rechsteiner, M. (1987). Purification of two high molecular weight proteases from rabbit reticulocyte lysate. *J Biol Chem*, 262(17), 8303-8313.
- Hunter, T. (1987). A thousand and one protein kinases. *Cell*, 50(6), 823-829.
- Joshi, V. and Jander, G. (2009). Arabidopsis methionine gamma-lyase is regulated according to isoleucine biosynthesis needs but plays a subordinate role to threonine deaminase. *Plant Physiol*, 151(1), 367-378.
- Kessler, F. and Schnell, D. (2009). Chloroplast biogenesis: diversity and regulation of the protein import apparatus. *Curr Opin Cell Biol*, 21(4), 494-500.
- Kessler, F. and Schnell, D. J. (2006). The function and diversity of plastid protein import pathways: a multilane GTPase highway into plastids. *Traffic*, 7(3), 248-257.
- Kikuchi, S.,Oishi, M.,Hirabayashi, Y.,Lee, D. W.,Hwang, I. and Nakai, M. (2009). A 1-megadalton translocation complex containing Tic20 and Tic21 mediates chloroplast protein import at the inner envelope membrane. *Plant Cell*, 21(6), 1781-1797.
- Kikuchi, Y.,Kojima, H. and Tanaka, T. (1999). Mutational analysis of the feedback sites of lysine-sensitive aspartokinase of *Escherichia coli*. *FEMS Microbiol Lett*, 173(1), 211-215.
- Kobe, B.,Jennings, I. G.,House, C. M.,Michell, B. J.,Goodwill, K. E.,Santarsiero, B. D.,Stevens, R. C.,Cotton, R. G. and Kemp, B. E. (1999). Structural basis of autoregulation of phenylalanine hydroxylase. *Nat Struct Biol*, 6(5), 442-448.
- Kovacs-Bogdan, E.,Soll, J. and Bolter, B. (2010). Protein import into chloroplasts: the Tic complex and its regulation. *Biochim Biophys Acta*, 1803(6), 740-747.
- Krupa, A.,Anamika and Srinivasan, N. (2006). Genome-wide comparative analyses of domain organisation of repertoires of protein kinases of *Arabidopsis thaliana* and *Oryza sativa*. *Gene*, 380(1), 1-13.
- Kumar Tewari, A. and Charan Tripathy, B. (1998). Temperature-stress-induced impairment of chlorophyll biosynthetic reactions in cucumber and wheat. *Plant Physiol*, 117(3), 851-858.
- Laber, B.,Maurer, W.,Hanke, C.,Grafe, S.,Ehlert, S.,Messerschmidt, A. and Clausen, T. (1999). Characterization of recombinant *Arabidopsis thaliana* threonine synthase. *Eur J Biochem*, 263(1), 212-221.
- Laemmli, U. K. (1970). Cleavage of structural proteins during the assembly of the head of bacteriophage T4. *Nature*, 227(5259), 680-685.
- Lamberti, G.,Drurey, C.,Soll, J. and Schwenkert, S. (2011). The phosphorylation state of chloroplast transit peptides regulates preprotein import. *Plant Signal Behav*, 6(12), 1918-1920.

- Lamberti, G., Gugel, I. L., Meurer, J., Soll, J. and Schwenkert, S. (2011). The cytosolic kinases STY8, STY17, and STY46 are involved in chloroplast differentiation in Arabidopsis. *Plant Physiol*, 157(1), 70-85.
- Lang, E. J., Cross, P. J., Mittelstadt, G., Jameson, G. B. and Parker, E. J. (2014). Allosteric ACTion: the varied ACT domains regulating enzymes of amino-acid metabolism. *Curr Opin Struct Biol*, 29, 102-111.
- Lee, Y. T. and Duggleby, R. G. (2002). Regulatory interactions in Arabidopsis thaliana acetohydroxyacid synthase. *FEBS Lett*, 512(1-3), 180-184.
- Leister, D. (2003). Chloroplast research in the genomic age. *Trends Genet*, 19(1), 47-56.
- Lochhead, P. A. (2009). Protein kinase activation loop autophosphorylation in cis: overcoming a Catch-22 situation. *Sci Signal*, 2(54), pe4.
- Lohkamp, B., McDermott, G., Campbell, S. A., Coggins, J. R. and Laphorn, A. J. (2004). The structure of Escherichia coli ATP-phosphoribosyltransferase: identification of substrate binding sites and mode of AMP inhibition. *J Mol Biol*, 336(1), 131-144.
- Luan, S. (2002). Tyrosine phosphorylation in plant cell signaling. *Proc Natl Acad Sci U S A*, 99(18), 11567-11569.
- Madison, J. T. and Thompson, J. F. (1988). Characterization of soybean tissue culture cell lines resistant to methionine analogs. *Plant Cell Rep*, 7(7), 473-476.
- Martin, T., Sharma, R., Sippel, C., Waegemann, K., Soll, J. and Vothknecht, U. C. (2006). A protein kinase family in Arabidopsis phosphorylates chloroplast precursor proteins. *J Biol Chem*, 281(52), 40216-40223.
- Mas-Droux, C., Curien, G., Robert-Genthon, M., Laurencin, M., Ferrer, J. L. and Dumas, R. (2006). A novel organization of ACT domains in allosteric enzymes revealed by the crystal structure of Arabidopsis aspartate kinase. *Plant Cell*, 18(7), 1681-1692.
- Mathur, S., Agrawal, D. and Jajoo, A. (2014). Photosynthesis: response to high temperature stress. *J Photochem Photobiol B*, 137, 116-126.
- May, T. and Soll, J. (2000). 14-3-3 proteins form a guidance complex with chloroplast precursor proteins in plants. *Plant Cell*, 12(1), 53-64.
- Mayer, M. P. and Bukau, B. (2005). Hsp70 chaperones: cellular functions and molecular mechanism. *Cell Mol Life Sci*, 62(6), 670-684.
- Meng, J., Wang, L., Wang, J., Zhao, X., Cheng, J., Yu, W., Jin, D., Li, Q. and Gong, Z. (2018). METHIONINE ADENOSYLTRANSFERASE4 Mediates DNA and Histone Methylation. *Plant Physiol*, 177(2), 652-670.
- Mitnaul, L. J. and Shiman, R. (1995). Coordinate regulation of tetrahydrobiopterin turnover and phenylalanine hydroxylase activity in rat liver cells. *Proc Natl Acad Sci U S A*, 92(3), 885-889.
- Nagy, P. L., Marolewski, A., Benkovic, S. J. and Zalkin, H. (1995). Formyltetrahydrofolate hydrolase, a regulatory enzyme that functions to balance pools of tetrahydrofolate and one-carbon tetrahydrofolate adducts in Escherichia coli. *J Bacteriol*, 177(5), 1292-1298.
- Nakrieko, K. A., Mould, R. M. and Smith, A. G. (2004). Fidelity of targeting to chloroplasts is not affected by removal of the phosphorylation site from the transit peptide. *Eur J Biochem*, 271(3), 509-516.
- Nester, E. W. and Jensen, R. A. (1966). Control of aromatic acid biosynthesis in Bacillus subtilis: sequential feedback inhibition. *J Bacteriol*, 91(4), 1594-1598.
- Nickel, C., Soll, J. and Schwenkert, S. (2015). Phosphomimicking within the transit peptide of pHCF136 leads to reduced photosystem II accumulation in vivo. *FEBS Lett*, 589(12), 1301-1307.
- Niyogi, K. K. (1999). PHOTOPROTECTION REVISITED: Genetic and Molecular Approaches. *Annu Rev Plant Physiol Plant Mol Biol*, 50, 333-359.
- Nolen, B., Taylor, S. and Ghosh, G. (2004). Regulation of protein kinases; controlling activity through activation segment conformation. *Mol Cell*, 15(5), 661-675.
- Paetzel, M., Karla, A., Strynadka, N. C. and Dalbey, R. E. (2002). Signal peptidases. *Chem Rev*, 102(12), 4549-4580.
- Pelech, S. (2006). Dimerization in protein kinase signaling. *J Biol*, 5(5), 12.

- Pfalz, J., Liebers, M., Hirth, M., Grubler, B., Holtzegel, U., Schroter, Y., Dietzel, L. and Pfannschmidt, T. (2012). Environmental control of plant nuclear gene expression by chloroplast redox signals. *Front Plant Sci*, 3, 257.
- Porra, R., Thompson, W. and Kriedemann, P. (1989). Determination of accurate extinction coefficients and simultaneous equations for assaying chlorophylls a and b extracted with four different solvents: verification of the concentration of chlorophyll standards by atomic absorption spectroscopy. *Biochem Biophys Acta*, 979, 384-394.
- Qbadou, S., Becker, T., Bionda, T., Reger, K., Ruprecht, M., Soll, J. and Schleiff, E. (2007). Toc64--a preprotein-receptor at the outer membrane with bipartite function. *J Mol Biol*, 367(5), 1330-1346.
- Qbadou, S., Becker, T., Mirus, O., Tews, I., Soll, J. and Schleiff, E. (2006). The molecular chaperone Hsp90 delivers precursor proteins to the chloroplast import receptor Toc64. *EMBO J*, 25(9), 1836-1847.
- Ravanel, S., Block, M. A., Rippert, P., Jabrin, S., Curien, G., Rebeille, F. and Douce, R. (2004). Methionine metabolism in plants: chloroplasts are autonomous for de novo methionine synthesis and can import S-adenosylmethionine from the cytosol. *J Biol Chem*, 279(21), 22548-22557.
- Ravanel, S., Gakiere, B., Job, D. and Douce, R. (1998). The specific features of methionine biosynthesis and metabolism in plants. *Proc Natl Acad Sci U S A*, 95(13), 7805-7812.
- Reddy, M. M. and Rajasekharan, R. (2007). Serine/threonine/tyrosine protein kinase from *Arabidopsis thaliana* is dependent on serine residues for its activity. *Arch Biochem Biophys*, 460(1), 122-128.
- Richardson, L. G., Paila, Y. D., Siman, S. R., Chen, Y., Smith, M. D. and Schnell, D. J. (2014). Targeting and assembly of components of the TOC protein import complex at the chloroplast outer envelope membrane. *Front Plant Sci*, 5, 269.
- Richmond, T. and Somerville, S. (2000). Chasing the dream: plant EST microarrays. *Curr Opin Plant Biol*, 3(2), 108-116.
- Romani, I., Manavski, N., Morosetti, A., Tadini, L., Maier, S., Kuhn, K., Ruwe, H., Schmitz-Linneweber, C., Wanner, G., Leister, D. and Kleine, T. (2015). A Member of the Arabidopsis Mitochondrial Transcription Termination Factor Family Is Required for Maturation of Chloroplast Transfer RNA^{Leu}(GAU). *Plant Physiol*, 169(1), 627-646.
- Rossel, J. B., Wilson, I. W. and Pogson, B. J. (2002). Global changes in gene expression in response to high light in *Arabidopsis*. *Plant Physiol*, 130(3), 1109-1120.
- Rudrabhatla, P., Reddy, M. M. and Rajasekharan, R. (2006). Genome-wide analysis and experimentation of plant serine/ threonine/tyrosine-specific protein kinases. *Plant Mol Biol*, 60(2), 293-319.
- Sauter, M., Moffatt, B., Saechao, M. C., Hell, R. and Wirtz, M. (2013). Methionine salvage and S-adenosylmethionine: essential links between sulfur, ethylene and polyamine biosynthesis. *Biochem J*, 451(2), 145-154.
- Schenk, P. M., Kazan, K., Wilson, I., Anderson, J. P., Richmond, T., Somerville, S. C. and Manners, J. M. (2000). Coordinated plant defense responses in *Arabidopsis* revealed by microarray analysis. *Proc Natl Acad Sci U S A*, 97(21), 11655-11660.
- Schertl, P., Danne, L. and Braun, H. P. (2017). 3-Hydroxyisobutyrate Dehydrogenase Is Involved in Both, Valine and Isoleucine Degradation in *Arabidopsis thaliana*. *Plant Physiol*, 175(1), 51-61.
- Schleiff, E., Soll, J., Sveshnikova, N., Tien, R., Wright, S., Dabney-Smith, C., Subramanian, C. and Bruce, B. D. (2002). Structural and guanosine triphosphate/diphosphate requirements for transit peptide recognition by the cytosolic domain of the chloroplast outer envelope receptor, Toc34. *Biochemistry*, 41(6), 1934-1946.
- Schnell, D. J., Blobel, G., Keegstra, K., Kessler, F., Ko, K. and Soll, J. (1997). A consensus nomenclature for the protein-import components of the chloroplast envelope. *Trends Cell Biol*, 7(8), 303-304.
- Schreiter, E. R., Sintchak, M. D., Guo, Y., Chivers, P. T., Sauer, R. T. and Drennan, C. L. (2003). Crystal structure of the nickel-responsive transcription factor NikR. *Nat Struct Biol*, 10(10), 794-799.

- Schuller, D. J., Grant, G. A. and Banaszak, L. J. (1995). The allosteric ligand site in the Vmax-type cooperative enzyme phosphoglycerate dehydrogenase. *Nat Struct Biol*, 2(1), 69-76.
- Schwenkert, S., Soll, J. and Bolter, B. (2011). Protein import into chloroplasts--how chaperones feature into the game. *Biochim Biophys Acta*, 1808(3), 901-911.
- Sjuts, I., Soll, J. and Bolter, B. (2017). Import of Soluble Proteins into Chloroplasts and Potential Regulatory Mechanisms. *Front Plant Sci*, 8, 168.
- Sun, W., Shahinas, D., Bonvin, J., Hou, W., Kimber, M. S., Turnbull, J. and Christendat, D. (2009). The crystal structure of Aquifex aeolicus prephenate dehydrogenase reveals the mode of tyrosine inhibition. *J Biol Chem*, 284(19), 13223-13232.
- Tang, H., Bowers, J. E., Wang, X., Ming, R., Alam, M. and Paterson, A. H. (2008). Synteny and collinearity in plant genomes. *Science*, 320(5875), 486-488.
- Thompson, J. R., Bell, J. K., Bratt, J., Grant, G. A. and Banaszak, L. J. (2005). Vmax regulation through domain and subunit changes. The active form of phosphoglycerate dehydrogenase. *Biochemistry*, 44(15), 5763-5773.
- Voigt, C., Oster, U., Bornke, F., Jahns, P., Dietz, K. J., Leister, D. and Kleine, T. (2010). In-depth analysis of the distinctive effects of norflurazon implies that tetrapyrrole biosynthesis, organellar gene expression and ABA cooperate in the GUN-type of plastid signalling. *Physiol Plant*, 138(4), 503-519.
- Waegemann, K. and Soll, J. (1996). Phosphorylation of the transit sequence of chloroplast precursor proteins. *J Biol Chem*, 271(11), 6545-6554.
- Zhang, X. P. and Glaser, E. (2002). Interaction of plant mitochondrial and chloroplast signal peptides with the Hsp70 molecular chaperone. *Trends Plant Sci*, 7(1), 14-21.

Acknowledgement

First, I would like to thank Prof. Jürgen Soll for giving me the opportunity to be a member of his group and for allowing me to conduct my studies in his laboratory.

I would also like to thank my supervisor PD Dr. Serena Schwenkert for her excellent and valuable supervision.

I would also like to thank Bettina Bölter for valuable suggestions for my experiments.

I would like to thank Prof. Jörg Nickelsen, Prof. Herwig Stibor, and Dr. Remino Zoschke for their advices during our annual thesis committee meetings.

Special thanks to current and former colleagues Roberto, Li, Tamara, Annabel, Melanie M, Melanie B, Kerstin S, Sebnem, and everyone else that contributed to my special experience here.

Additional thanks goes to my past supervisors Prof. Jürgen Kleine-Vehn, Dr. David Scheuring, and Prof. Dr. Matt Dalby for their support throughout my academic path.

Finally, I would like to thank my family and friends for their constant support and encouragement.

Curriculum vitae

Personal Details

Given Name: Ahmed Eisa
 Date of birth: 02. January 1989
 Place of birth: Khartoum, Sudan
 Citizenship: Austria

Education & Civil Service

July 2016 - December 2019

Ludwig-Maximillan University, Munich, Germany
 Supervisor: PD Dr. Serena Schwenkert
 Prof. Dr. Jürgen Soll Laboratory
 Department Biology I - Plant Sciences

Doctoral Studies in Biology (Dr. rer nat)

October 2012 - November 2015

University Of Vienna, Vienna, Austria
 Masters of Science Degree (MSc)
 Molecular Biology - Biochemistry

January 2012 - June 2012

Austrian Federal Army, Vienna, Austria
 Conscription Military Service - National Guard

September 2007 - May 2011

University Of Glasgow, Glasgow, United Kingdom
 Bachelor of Science Honors degree (BSc Hons)
 Biomedical Sciences - Biochemistry

February 1999 – June 2007

Vienna International School, Vienna, Austria
International Baccalaureate - Certificate
 Subjects: English, German, Arabic, History,
 Mathematics, Chemistry, Biology.

Scientific Contributions

Publications

Eisa A, Bölter B, Schwenkert S. 'The ACT domain in chloroplast precursor-phosphorylating STY kinases binds metabolites and allosterically regulates kinase activity', *Journal of Biological Chemistry*, 2019.

Kaiser S, Eisa A, Kleine-Vehn J, Scheuring D. 'NET4 modulates the compactness of vacuoles in Arabidopsis thaliana', *International Journal of Molecular Sciences*, 2019.

Guan L, Denkert N, Eisa A, Lehmann M, Sjuts I, Weiberg A, Soll J, Meinecke M, Schwenkert S. 'JASSY - a Chloroplast Outer Membrane Protein Required for Jasmonate Biosynthesis', *Proceedings of the National Academy of Sciences (PNAS)*, 2019.

Scheuring D., Löffke C., Krüger F., Kittelmann M, Eisa A., Hughes L., Smith RS, Hawes C., Schumacher K., Kleine-Vehn J.' Actin-dependent cellular occupancy of the vacuole determines auxin-induced growth repression', *Proceedings of the National Academy of Sciences (PNAS)*, 2015.

Conferences

04 – 08.08.2019
 Irsee, Germany.

Acclimation & Chloroplast Biology: from Genes to Systems
 TRR 175 The Green Hub - Central Coordinator of Acclimation in Plants

23 - 25.09. 2018
 Bremerhaven, Germany.

XIX. Annual Meeting German section of the International Society of Endocytobiology (ISE-G)

9-10.07. 2018
 Vienna, Austria.

V. International Conference in Plant Physiology & Biochemistry
 Vienna International Science Conferences & Events Association (VISCEA)

Veröffentlichung

Teile dieser Arbeit sind zur Veröffentlichung vorgesehen. Folgendes Manuskript ist zur Veröffentlichung eingereicht:

Eisa A, Malenica K, Schwenkert S, Bölter B.' High light acclimation induces chloroplast precursor phosphorylation and reduces import efficiency', In review, 2019.

Eidesstattliche Versicherung

Ich versichere hiermit an Eides statt, dass die vorgelegte Dissertation von mir selbständig und nur unter Verwendung der angegebenen Hilfsmittel und Quellen angefertigt wurde.

München, den 16.12.2019

Ahmed Eisa